The Journal of Immunology

Integrin Cross-Talk Regulates the Human Neutrophil Response to Fungal β-Glucan in the Context of the Extracellular Matrix: A Prominent Role for VLA3 in the Antifungal Response

Courtney M. Johnson, Xian M. O'Brien, Angel S. Byrd, Valentina E. Parisi, Alex J. Loosely, Wei Li, Hadley Witt, Hafeez M. Faridi, Craig T. Lefort, Vineet Gupta, Minsoo Kim and Jonathan S. Reichner

J Immunol published online 16 November 2016
http://www.jimmunol.org/content/early/2016/11/15/jimmunol.1502381

The Journal of Immunology is published twice each month by The American Association of Immunologists, Inc., 9650 Rockville Pike, Bethesda, MD 20814-3994.

Print ISSN: 0022-1767 Online ISSN: 1550-6606.

Published November 16, 2016, doi:10.4049/jimmunol.1502381

Integrin Cross-Talk Regulates the Human Neutrophil Response to Fungal β-Glucan in the Context of the Extracellular Matrix: A Prominent Role for VLA3 in the Antifungal Response

Courtney M. Johnson,[*,†,‡,1] Xian M. O'Brien,[*,†,1] Angel S. Byrd,[*,†,‡] Valentina E. Parisi,[*,‡] Alex J. Loosely,[§] Wei Li,[*] Hadley Witt,[*,†,‡] Hafeez M. Faridi,[¶] Craig T. Lefort,[*,†] Vineet Gupta,[¶] Minsoo Kim,[‖] and Jonathan S. Reichner[*,†,‡]

Candida albicans **infection produces elongated hyphae resistant to phagocytic clearance compelling alternative neutrophil effector mechanisms to destroy these physically large microbial structures. Additionally, all tissue-based neutrophilic responses to fungal infections necessitate contact with the extracellular matrix (ECM). Neutrophils undergo a rapid, ECM-dependent mechanism of homotypic aggregation and NETosis in response to *C. albicans* mediated by the β_2 integrin, complement receptor 3 (CR3, CD11b/CD18, $\alpha_M\beta_2$). Neither homotypic aggregation nor NETosis occurs when human neutrophils are exposed either to immobilized fungal β-glucan or to *C. albicans* hyphae without ECM. The current study provides a mechanistic basis to explain how matrix controls the antifungal effector functions of neutrophils under conditions that preclude phagocytosis. We show that CR3 ligation initiates a complex mechanism of integrin cross-talk resulting in differential regulation of the β_1 integrins VLA3 ($\alpha_3\beta_1$) and VLA5 ($\alpha_5\beta_1$). These β_1 integrins control distinct antifungal effector functions in response to either fungal β-glucan or *C. albicans* hyphae and fibronectin, with VLA3 inducing homotypic aggregation and VLA5 regulating NETosis. These integrin-dependent effector functions are controlled temporally whereby VLA5 and CR3 induce rapid, focal NETosis early after binding fibronectin and β-glucan. Within minutes, CR3 undergoes inside-out auto-activation that drives the downregulation of VLA5 and the upregulation of VLA3 to support neutrophil swarming and aggregation. Forcing VLA5 to remain in the activated state permits NETosis but prevents homotypic aggregation. Therefore, CR3 serves as a master regulator during the antifungal neutrophil response, controlling the affinity states of two different β_1 integrins, which in turn elicit distinct effector functions.** ***The Journal of Immunology*****, 2017, 198: 000–000.**

Deep-seated fungal infections are a major cause of morbidity and mortality due largely to a growing patient population with clinically impaired host defenses (1–6). Many cases are secondary to immunosuppression following organ transplantation, cancer chemotherapy, and AIDS, although trauma and burn patients, patients with diabetes, and the elderly are particularly susceptible as well (1, 7). Increasingly complex surgical procedures have led to the increased use of invasive measures such as i.v. catheters and hyperalimentation, which further contribute to the risk of acquiring candidiasis, particularly in patients maintained in the surgical intensive care unit for extended periods of time during recovery (8–10). *Candida* infection was reported to be remarkably high in non-trauma emergency surgical patients with prolonged hospital stays reaching a rate of 21.7/100 discharges, higher than other established high-risk patient populations (11). If the infection progresses to invasive, systemic candidiasis, the associated mortality ranges between 63–85% in untreated cases and 33–54% in those receiving appropriate antifungal therapy (12).

Neutrophils are the primary effector cells in promoting destruction and preventing dissemination of fungal pathogens (13–15). A low peripheral blood neutrophil count or a genetic defect in neutrophil function is sufficient to create host susceptibility for severe invasive fungal infections (16). Dimorphic fungi such as *C. albicans* switch in vivo between the single-cell blastoconidia form and the elongated hyphal form (17). Given its relatively small size, the single-cell form of *C. albicans* can be cleared by host neutrophils via phagocytosis. However, the large size of the hyphae obviates ingestion and thereby poses a challenge to the antifungal defense mechanisms available to the neutrophil (18).

Because mycotic infections occur within tissues, the response of extravasated neutrophils to fungal pathogens must take place in the context of the extracellular matrix (ECM). Recent work from this

*Division of Surgical Research, Department of Surgery, Rhode Island Hospital, Providence, RI 02903; [†]Warren Alpert Medical School, Brown University, Providence, RI 02912; [‡]Graduate Program in Pathobiology, Brown University, Providence, RI 02912; [§]Department of Physics, Brown University, Providence, RI 02912; [¶]Department of Internal Medicine, Rush University Medical Center, Chicago, IL 60612; and [‖]David H. Smith Center for Vaccine Biology and Immunology, Department of Microbiology and Immunology, University of Rochester, Rochester, NY 14642

[1]C.M.J. and X.M.O. contributed equally to this work.

ORCIDs: 0000-0001-5906-0612 (C.M.J.); 0000-0003-0958-5343 (X.M.O.); 0000-0002-3721-784X (W.L.); 0000-0003-4390-7959 (H.M.F.); 0000-0003-3100-877X (C.T.L.); 0000-0001-6987-2550 (V.G.); 0000-0002-7349-6321 (J.S.R.).

Received for publication November 9, 2015. Accepted for publication October 20, 2016.

This work was supported by National Institutes of Health Grants GM066194 (J.S.R.), HL125265 (J.S.R. and M.K.), and DK106512, HL109582, and DK084195 (V.G.) and by United Negro College Fund/Merck Graduate Science Research Dissertation Fellowships (A.S.B. and C.M.J.). Work was also supported by funds from the Department of Surgery, Rhode Island Hospital.

Address correspondence and reprint requests to Dr. Jonathan S. Reichner, Department of Surgery, Rhode Island Hospital, 593 Eddy Street, Providence, RI 02903. E-mail address: Reichner@Brown.edu

Abbreviations used in this article: CR3, complement receptor 3; ECM, extracellular matrix; Fn, fibronectin; FRET, fluorescence resonance energy transfer; LA1, leukadherin-1; MFI, mean fluorescence intensity; NET, neutrophil extracellular trap; ORB, octadecyl rodamine B; PAMP, pathogen-associated molecular pattern; SEM, scanning electron microscopy.

laboratory demonstrated a significant regulatory role for ECM in mediating the antifungal response of neutrophils (19). Specifically, we found that fibronectin (Fn) was required for neutrophil swarming and homotypic aggregation and a rapid release of neutrophil extracellular traps (NETs) with exposure to either immobilized soluble β-glucan or *C. albicans* hyphae. Neutrophil aggregation and NET release did not occur in response to either immobilized β-glucan, *C. albicans* hyphae, or Fn alone. The current study was undertaken to provide a mechanistic explanation for the coordinated response to the fungal pathogen associated molecular pattern (PAMP) β-glucan and the matrix protein Fn.

On human neutrophils, complement receptor 3 (CR3, CD11b/CD18, $\alpha_M\beta_2$), a β_2 integrin, serves as a pattern recognition receptor for the fungal PAMP β-glucan (20, 21). Our previous work has shown that neutrophil clustering and NETosis to β-glucan in the context of Fn requires CR3, but not dectin-1, and is independent of respiratory burst (19). CR3 is a unique surface receptor capable of recognizing ligands at two spatially distinct domains, the I-domain and the lectin-like domain. The promiscuous I-domain recognizes many ligands including Fn, fibrinogen, and ICAM-1 (22). The lectin-like site has been shown to bind β-glucan (23). The simultaneous binding of both I-domain ligand and lectin-like domain ligand has been proposed to regulate cellular function not seen with ligation of either domain alone. In this study, we report a novel, complex, and temporally regulated integrin cross-talk pathway in which dual ligation of CR3 signals the differential regulation of VLA3 ($\alpha_3\beta_1$) and VLA5 ($\alpha_5\beta_1$), β_1 integrins not often associated with antifungal activity. Neutrophil swarming was determined by activated VLA3 whereas NETosis required activated VLA5; the activation state of CR3 regulated the activation states of both VLA3 and VLA5. Findings are consistent with a two-stage temporal model where VLA5 and CR3 are initially activated by ligand binding upon contact with Fn and fungal β-glucan leading to rapid, matrix-dependent NET formation. Over time, dually ligated CR3 undergoes an inside-out auto-activation that drives the downregulation (suppression) of VLA5 and the upregulation (activation) of VLA3 to allow for neutrophil swarming and cluster formation. If VLA5 is maintained in a high state of activation, VLA3 cannot be engaged. To our knowledge, these data provide the first direct evidence for integrin cross-talk between the β_2 integrin CR3 to the β_1 integrins VLA3 and VLA5 in human neutrophils exposed to fungal determinants. Taken together with previous reports, this study highlights the essentiality of considering the regulatory role of the ECM and cognate integrins in efforts to understand host defense as it occurs within a tissue microenvironment.

Materials and Methods

Reagents

Abs used were as follows: blocking anti-CD11b (clone 44abc) hybridoma from American Type Culture Collection (Manassas, VA), APC-conjugate IgG (BioLegend, San Diego, CA), APC-conjugate CD11b (CBRM1/5; BioLegend), human integrin alpha5/CD49e Ab (clone P1D6; R&D Systems, Minneapolis, MN), Mouse IgG1 Isotype Control (R&D Systems), Mouse anti-human integrin α_3 (VLA3) preservative-free mAb (clone M-KID2; EMD Millipore, Temecula, CA), anti-VLA6 (NKI-GoH3; EMD Millipore, Temecula, CA), FITC-conjugated anti-CD11b (CBRM1/5; BioLegend), FITC-conjugated mouse IgG1 (679.1Mc7; Beckman Coulter Brea, CA), and FITC-conjugated anti-CD11b (ICRF44; Ancell, Bayport, MN). Anti-alpha5 (preservative-free) (SNAKA51; EMD Millipore), anti-Integrin alpha3, azide-free (ASC-1; EMD Millipore), and pharmaceutical-grade purified, endotoxin-free, soluble yeast β-glucan (ImPrime PGG) was kindly provided by Biothera (Eagan, MA). This is a β-glucan(1, 3) (1, 6) from the cell wall of *Saccharomyces cerevisiae* with an average m.w. of 150 kDa and 4.1% branching (24). The β-glucan preparation contained no more than 0.02% protein, 0.01% mannan, and 1% glucosamine. Purified, endotoxin-free human Fn was from BD Biosciences (Bedford, MA). Dulbecco's PBS, Lebovitz's L15 medium (L-15), HBSS, and Sytox Green were from Invitrogen (Carlsbad, CA). Accutase was from Innovative Cell Technologies (San Diego, CA). Leukadherin-1 (LA1), a small molecule CR3 receptor agonist with function-blocking properties, was a gift from Dr. Vineet Gupta, Rush Medical Center, Chicago, IL. VLA3 blocking peptide (LXY1) and the β_2 integrin allosteric antagonist (XVA143) were from Dr. Minsoo Kim, University of Rochester, Rochester, NY. All other reagents were obtained from Sigma-Aldrich (St. Louis, MO), unless otherwise indicated, and were of the highest quality available.

Neutrophil isolation

Blood was obtained from healthy human volunteers with approval of the Rhode Island Hospital Institutional Review Board. Blood was collected in EDTA-containing Vacutainer tubes (BD Biosciences, San Jose, CA) and used within 5 min of venipuncture. Histopaque-1077 was used for initial cell separation followed by sedimentation through 3% dextran (400–500 kDa molecular mass). Contaminating erythrocytes were removed by hypotonic lysis, yielding a 95% pure neutrophil preparation of 90% viability by trypan dye exclusion. Neutrophils were suspended in HBSS (without Ca^{2+}/Mg^{2+}) and placed on ice until use.

Neutrophil adhesion assay

Six-well tissue culture plates (Fisher Scientific, Waltham, MA) were coated overnight at 4°C with Fn at a concentration of 6 μg/ml in TBS (25 mM Tris, 150 mM NaCl) pH 9.0 and/or 1 mg/ml β-glucan. Plates were moved to 37°C for 1 h, washed twice with PBS, and air dried. Neutrophils were resuspended to a concentration of 3.5×10^6 cells/ml in L-15 medium supplemented with 2 mg/ml glucose and 2 ml was added to each well. Where indicated, cells were preincubated with 25 μg/ml blocking or activating mAb or isotype control on ice for 30 min. Cells were pretreated on ice with 10^{-9} M fMLP for 20 min and 1 mM Mn^{2+} was added to cells immediately before plating. Cells were exposed to either Fn alone or Fn + β-glucan for 30 min at 37°C. In a subset of experiments, 150 U/ml of DNase I was added at 0, 10, or 25 min, as noted. Cells were then imaged and scored for cluster formation and NETosis or harvested for FACS analysis.

Scanning electron microscopy

Samples for scanning electron microscopy (SEM) were fixed by gently layering 2.5% glutaraldehyde in 0.15 M sodium cacodylate buffer, rinsed with buffer and post fixed with 1% osmium tetroxide. Slides were rinsed, dehydrated and covered with resin and placed over Epox 812 filled slide-duplicating molds (Electron Microscopy Sciences, Hatfield, PA) overnight. Following dehydration in ethanol, samples were subsequently dried in a critical point dryer. The samples were then coated with 20 nm of gold palladium (60:40) in an Emitech K550 sputter coater (Emitech, Ashford, U.K.). Cells were imaged with a Hitachi S-2700 scanning electronic microscope (Hitachi High Technologies America, Pleasanton, CA) and collected with Quartz PCI software (Quartz Imaging, Vancouver, BC).

Quantification of neutrophil cluster formation

Cluster formation was quantified using custom MatLab software. Multiple images were taken per well and clusters of neutrophils were identified by eye as regions of interconnected or overlapping cells contained within a field of view (most fields of view were 410 × 410 mm). Only cluster regions with areas >400 mm^2 were considered, approximately the size of four tiled, non-overlapping neutrophils. To maximize consistency, a single person was used to identify every cluster region in each field of view captured. To minimize human bias, experimental conditions associated with each field of view were coded and the person doing the analysis was blinded. Fields of view were numerically characterized by the number of clusters per square millimeter and the average area of each cluster in square micrometers. Data sets from each well were averaged and all wells for each condition were ensemble averaged and plotted as average clusters per millimeter (*x*-axis) versus average cluster area in square micrometer (*y*-axis) per condition. Ellipses represent 2D-SEM. Data represents 3–20 wells per condition.

Visualization and quantification of neutrophil NETs

Neutrophils were adhered as previously described to plates coated with Fn ± β-glucan. NETs were visualized on adherent neutrophils by addition of 5 μM Sytox green and multiple images were taken per well. To minimize bias, experimental conditions associated with each field of view were coded and the person doing the analysis was blinded. Images were thresholded using the default thresholding algorithm in ImageJ (National Institutes of Health, Bethesda, MD) and gated to include NETs and exclude nuclei. NET

formation was quantified as a percentage area of the totaled imaged field. Well averages were ensemble averaged to generate this data. Data represents 3–20 wells per condition.

Microscopy

Images were captured using a Nikon TE-2000U inverted microscope (Nikon, Melville, NY) coupled to an iXonEM+ 897E back illuminated EMCCD camera (Andor, Belfast, U.K.) outfitted with a Bioptechs (Butler, PA) stage heater and 20 ×, Nikon Plan Apochromat objective. Bright field images were captured using Elements software (Nikon). For fluorescence microscopy, a xenon lamp illuminated cells through a 33 mm ND4 filter and 20 × Nikon Plan Apochromat objective using a Nikon B2-A long pass emission filter set cube.

FACS analysis

Following isolation procedure, neutrophils were resuspended to a concentration of 3.5×10^6 cells/ml in L-15 medium supplemented with 2 mg/ml glucose, and 2 ml was added to each well. Where indicated, cells were preincubated with integrin specific mAbs, peptides, or small molecules and vehicle or isotype controls. Cells were pretreated on ice with 10^{-9} M fMLP for 20 min and 1 mM Mn^{2+} was added to cells immediately before plating. Cells were exposed to either Fn alone or Fn + β-glucan for 30 min at 37˚C. Following incubation time, 2 ml of Accutase and 150 U/ml DNase I (Sigma-Aldrich) was added to each well and the plate was incubated at 37˚C for an additional 7 min. To remove cells, the contents of wells were first pipetted up-and-down with serological pipettes, then gently scraped from the well surface using cell scrapers (Costar, Corning, NY) and collected in 15 ml conical tubes. Wells were examined by microscope and 1 ml of L-15 was added, then the wells were rescraped if needed. Cells were spun down at 4˚C for 10 min at 1400 rpm in a clinical centrifuge and resuspended at 1×10^7 cells/ml in BSS+ buffer (0.1% BSA, 1 mM $CaCl_2$, 1 mM $MgCl_2$) 100 μl cell aliquots were incubated with FITC-IgG control (10 μg/ml), FITC-ICRF44 (9.8 μg/ml), FITC-CBRM1/5 (15 μg/ml), FITC-ASC-1(10 μg/ml), FITC-P1D6 (10 μg/ml), or FITC-SNAKA51 (2.5 μg/ml) and Fc block (Accurate Chemical, Westbury, NY) for 60 min on ice at 4˚C in foil. (Unconjugated mAb were labeled using a Molecular Probes Alexa fluor 488 Ab labeling kit per manufacturer's instructions.) Cells were washed three times with BSS+ at 4˚C and resuspended in 1% paraformaldehyde in PBS. Data was acquired on either a BD FACScan (Becton, Dickinson and Company, Franklin Lakes, NJ) using Lysis II software or by the Brown University Flow Cytometry and Sorting Facility on a BD FACSAria IIu using FACS DiVa software. Analysis was performed in FlowJo software (FlowJo, Ashland, OR) gating on neutrophils.

FACS-based fluorescence resonance energy transfer assay for extracellular extension of CR3 or VLA3

Experiments were performed as described in previous literature (25, 26). Briefly, neutrophil adhesion assays were performed as described above. A total of 2 ml of thawed Accutase and 150 U/ml DNaseI (Sigma-Aldrich) were added per well, the sides of the plates were tapped for 30 s, and placed at 37˚C for 7 min. To remove cells, contents of wells were first pipetted up-and-down with serological pipettes, then gently scraped from the well surface using cell scrapers (Costar), and collected in 15 ml conical tubes. Wells were examined by microscope and 1 ml of L15 was added and wells rescraped if needed. Cells were spun down at 4˚C for 10 min at 1400 rpm in a clinical centrifuge and resuspended at 1×10^7 cells/ml in BSS+ buffer (0.1% BSA, 1 mM $CaCl_2$, 1 mM $MgCl_2$) 100 μl cell aliquots were incubated with FITC-IgG control (10 μg/ml), FITC-ICRF44 (9.8 μg/ml), FITC-CBRM1/5 (15 μg/ml), or FITC-ASC-1 (10 μg/ml) for 50 min with rotation at 4˚C in foil. Cells were washed three times with BSS+ at 4˚C and split into four 125 μl aliquots in FACS compatible snap cap tubes on ice. Octadecyl rodamine B (ORB) was added to a final volume of 250 μl and concentrations of 0, 75, 200, and 400 nM. Samples were incubated on ice for 20 min and data were acquired by the Brown University Flow Cytometry and Sorting Facility on a BD FACSAria IIu using FACS DiVa software. Analysis was performed in FlowJo software gating on neutrophils.

Statistical analysis

Data was pooled from a minimum of three independent experiments representing at least three different donors, as indicated. ANOVA analysis with Newman–Keuls post hoc analysis or paired-sample Student *t* test as appropriate were performed using MatLab (Mathworks, Natick, MA) or Excel (Microsoft, Redmond, WA) running the statistiXL data package (statistiXL, Nedlands, Australia). The null hypothesis was rejected if $p < 0.001$.

Results

Homotypic aggregation of neutrophils in response to C. albicans *hyphae or immobilized β-glucan in the context of fibronectin*

C. albicans infection instilled into a rat kidney shows robust aggregation of neutrophils (stained in red using an anti-neutrophil Ab) about a hyphal filament [stained in green using an anti-β-glucan Ab specific for β- (1–3)- and β- (1–6)-linked glucose (Fig. 1, left panel)]. This characteristic neutrophil aggregation around fungal hyphae is also observed in vitro when neutrophils are coincubated with hyphae that have been elaborated on surfaces coated with Fn (Fig. 1, center panel). When this in vitro system is reduced to its minimal recognition elements of immobilized fungal β-glucan and Fn, cluster formation is conserved (Fig. 1, right panel). We have previously used these in vitro systems to characterize a rapid, matrix-dependent NET response of human neutrophils to fungal β-glucan (19). This study uses these model systems to characterize the integrin regulation of neutrophil cluster formation and NETosis to provide a mechanistic explanation for the dependence of matrix for the response to a fungal PAMP or hyphal filaments.

Homotypic aggregation on Fn + β-glucan is dependent on CR3 and VLA3 and independent of VLA5

To identify the specific integrins involved in neutrophil aggregation, human neutrophils were pretreated on ice with 10^{-9} M fMLP and incubated for 30 min at 37˚C on tissue culture plastic coated with either 6 μg/ml Fn (Fn alone) or 6 μg/ml Fn + 1 mg/ml β-glucan (Fn + β-glucan) in L-15 supplemented with 2 mg/ml glucose and 1 mM Mn^{++}. Previously, we showed that these conditions were optimal for primed neutrophils to exhibit rapid, reactive oxygen species-independent NETosis and homotypic aggregation. To identify integrins required for NET release and/or aggregation, neutrophils were additionally pretreated either with specific blocking mAbs to CR3 (clone 44abc), VLA5 (P1D6), VLA3 (M-KID2), or VLA6 (NKI-GoH3). Confirming our previous report, Ab blocking of CR3 blocked cluster formation (Fig. 2A). Surprisingly, we found that blocking VLA5, the canonical Fn receptor, had no effect on aggregation despite the presence of Fn in the assay, but blocking VLA3 completely inhibited cluster formation (Fig. 2A). VLA6 had no effect on clustering. Quantification of aggregate formation as average number of clusters per millimeter versus average area of clusters confirmed significant inhibition of neutrophil clusters in response to Fn + β-glucan to levels indistinguishable from Fn alone upon Ab blocking of either CR3 or VLA3 ($p < 0.001$), but with no significant change in cluster formation upon Ab blocking with isotype control (data not shown), VLA5, or VLA6 (Fig. 2B). The VLA5 independence of aggregate formation was confirmed using a second VLA5-blocking mAb AF1864 (data not shown).

CR3 adhesion to Fn + β-glucan drives its inside-out auto-activation

Given that CR3 is the dominant receptor for β-glucan recognition by human neutrophils, we sought to understand whether CR3 expression and activation state was differentially modulated on Fn+β-glucan versus Fn alone. Using flow cytometric analysis, CR3 surface expression and activation was quantified after adhesion on Fn ± β-glucan. Using a CR3 expression reporter Ab (ICRF44), no significant difference in CR3 surface expression was found as a function of ligand exposure (Fig. 2C, top panel). Using a CR3 activation reporter Ab, (CBRM 1/5), a significant increase in CR3 activation on Fn + β-glucan versus Fn alone was identified (Fig. 2C, bottom panel). This increase was lost on Fn +β-glucan when CR3 was blocked (Fig. 2C) supporting a mechanism of inside-out auto-activation of CR3 on Fn + β-glucan.

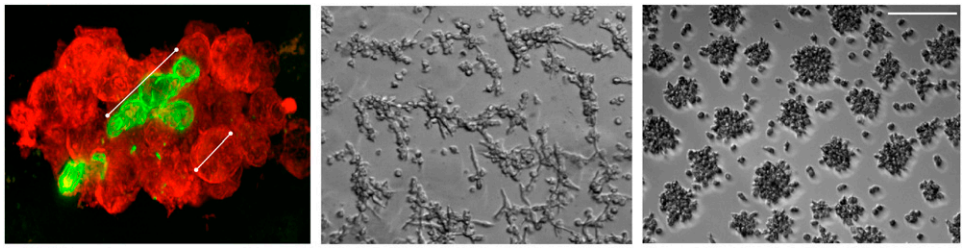

FIGURE 1. Immobilized β-glucan + Fn supports neutrophil aggregation as seen in vivo in response to intact hyphae in tissue. Left panel, *C. albicans* infection within a rat kidney shows robust aggregation of neutrophils (stained in red with an anti-neutrophil Ab) about a hyphal filament [stained in green using an anti-β-glucan Ab specific for β-(1–3), β-(1–6)-linked glucose]. Center panel, Aggregation also forms in vitro on intact *C. albicans* hyphae elaborated on Fn; original magnification ×20, bright field image. Right panel, β-glucan immobilized with Fn supports robust neutrophil aggregation; original magnification ×20, bright field image. Bar, 100 μm.

CR3 surface expression and activation on neutrophils was quantified after adhesion on Fn ± β-glucan in the presence or absence of VLA3 or VLA5 blocking mAbs (Fig. 2D). After 30 min incubation, neutrophils were isolated and stained with directly conjugated mAbs for both total CR3 (ICRF44) and a CR3 activation specific epitope (CBRM1/5), and assayed by FACS. The average ratio of the mean fluorescence intensity (MFI) for cells adhered to Fn alone versus cells adhered to Fn + β-glucan showed no significant increase in CR3 expression or activation on Fn + β-glucan after VLA3 or VLA5 blocking. That blockade of the β_1 integrins does not affect CR3 expression or activation suggests that the integrin cross-talk pathway under study takes place in the β_2-to-β_1, but not in the β_1-to-β_2, direction.

Neutrophil homotypic aggregation and NETosis are dependent on CR3 but are differentially regulated with VLA3 driving homotypic aggregation and VLA5 driving NET formation

After identifying differential roles for VLA3 and VLA5 in neutrophil clustering, we determined the role of these β_1 integrins in CR3-mediated rapid NET formation. Neutrophils were preincubated with blocking Abs to CR3 (clone 44abc), VLA3 (M-KID2), or VLA5 (P1D6) and then allowed to adhere to Fn or Fn + β-glucan-coated surfaces and incubated at 37˚C for 30 min, as above. NET formation was visualized using the cell impermeable DNA intercalating dye, Sytox green. Whereas CR3 was required for both cluster formation and NETosis to Fn + β-glucan, VLA3 engagement was required only for cluster formation and VLA5 was required only for NET production (Figs. 2A, 2B, 3A). Indeed, when NETs were quantified as an average percentage area of the total imaged field, VLA5 blocking significantly reduced NET formation to levels indistinguishable from either CR3 blocking or Fn alone, whereas VLA3 blocking did not significantly reduce NET formation (Fig. 3B). Scanning electron microscopy of neutrophils on Fn + β-glucan confirm of the presence of DNA fibril structures between aggregated cells (Fig. 3C, arrowheads) supporting the presence of extracellular DNA visualized by Sytox green staining of cells on Fn + β-glucan. These data support the hypothesis that CR3-dependent neutrophil cluster formation and NET response to Fn + β-glucan are decoupled with VLA5 being required for NETosis and VLA3 for homotypic aggregation.

Dissolution of NETs by DNase I disrupts early, but not late, neutrophil clusters. Neutrophil clusters form in the absence of intact NET structures. In a previous study, we reported that treatment with DNase I could dissolve Sytox green-staining NET structures and disrupt neutrophil clusters on Fn + β-glucan, which was consistent with the hypothesis that the NET structures played a physical role in seeding the neutrophil clusters (19). We now show in Fig. 3A that the CR3-dependent cluster formation and NET response to Fn + β-glucan are decoupled. To place this finding in the context of our previous work, we examined the temporal and longitudinal influence of DNase I in the formation of neutrophil clusters on Fn + β-glucan. Neutrophils were allowed to adhere to Fn + β-glucan–coated surfaces and incubated at 37˚C, as above. After 30 min, in the absence of DNase, NETs can be visualized with Sytox green at the center of neutrophil aggregates (Fig. 4, first column). If we allow the neutrophils to incubate at 37˚C for 10 min, early clusters can be visualized aggregating around NETotic foci (Fig. 4, second column, top panel). Addition of DNase I dissolved both Sytox-green staining NET structures and neutrophil clusters within 30 s (Fig. 4, second column, center panel). After an additional 20 min incubation, clusters were reformed in similar field locations in the absence of physical NET structures (Fig. 4, second column, bottom panel). Addition of DNase I after 25 min dissolved NET structures but mature clusters were not disrupted and persisted at 30 min (Fig. 4, third column). If DNase I is included in the assay medium from time 0 min and NET structures are not allowed to persist, cluster formation is still observed (Fig. 4, fourth column). These data suggest that although at early time points NETs can support the aggregation of neutrophils, the physical NET structures can be decoupled from neutrophil cluster formation.

A CR3 agonist leukadherin-1, which decouples CR3 binding from some downstream signaling, supports NET formation but partially inhibits cluster formation. Integrin affinity blocker, XVA143, blocks both cluster formation and NETosis

To further interrogate the role of CR3 identified in our Ab blocking studies, neutrophils were pretreated with either a small molecule CR3 agonist, LA1 or small molecule β_2 allosteric antagonist, XVA143 (XVA). The XVA antagonist binds to the β_2 I domain MIDAS near a key regulatory interface with the α I domain and blocks communication of conformational change to the I domain and at the same time inducing conformational rearrangements elsewhere in the integrin, including swing-out of the hybrid domain, resulting in an extended conformation with an inactive I domain (27, 28). Cluster formation and NETosis in response to Fn + β-glucan was completely abrogated in neutrophils pretreated with 10 μM XVA antagonist (Fig. 5). This indicates that the low affinity I domain conformation of CR3 does not support aggregate or NET formation. Interestingly, we found that neutrophils pretreated with 15 μM LA1, a small molecule CR3 agonist that prevents CR3 from leaving its high affinity conformation while decoupling the receptor from some of its intracellular signaling (29), showed significantly decreased neutrophil clusters in both number and area (Fig. 5A, 5C) but had no significant effect on NETosis (Fig. 5A, 5B). These data indicate that flexibility in the conformational state of CR3 determines neutrophil cluster formation and supports the involvement of CR3 intracellular signaling in

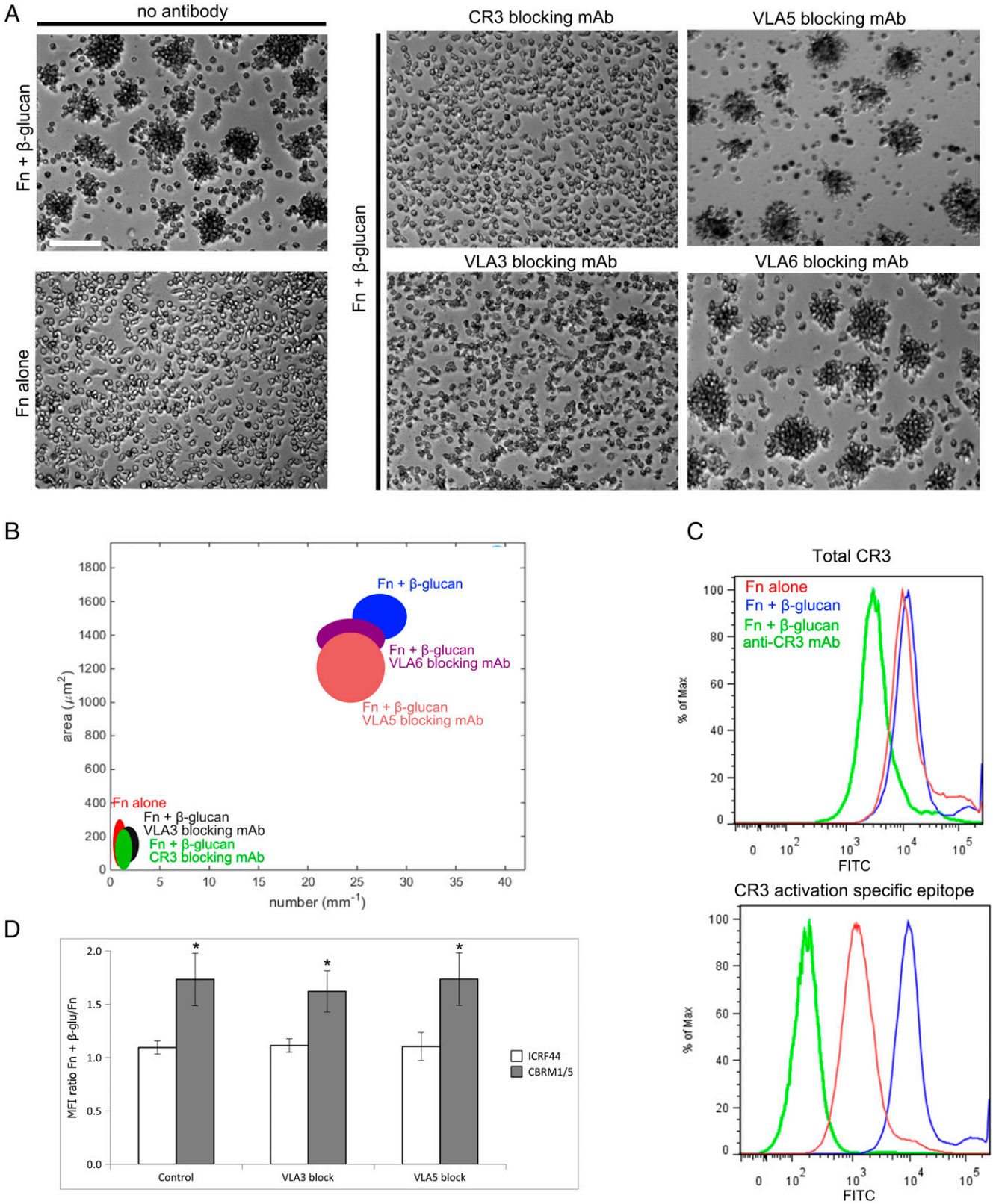

FIGURE 2. Neutrophil clustering on Fn + β-glucan is dependent on CR3 and VLA3. (**A**) Human neutrophils, pretreated on ice with 10^{-9} M fMLP, were incubated at 37°C on tissue culture plastic coated with either 6 μg/ml Fn (Fn alone) or 6 μg/ml Fn + 1 mg/ml β-glucan (Fn + β-glucan) in L-15 supplemented with 2 mg/ml glucose and 1 mM Mn^{++}. Where indicated, neutrophils were additionally pretreated either with specific blocking mAbs to CR3 (clone 44abc), VLA5 (P1D6), VLA3 (MKID-2) or VLA6 (NKI-GoH3). After 30 min incubation, cells were fixed and multiple images were acquired per well. Bright field images acquired at original magnification ×20; bar, 100 μm. (**B**) Neutrophil cluster formation was quantified using ImageJ and custom MatLab software and plotted as average clusters per millimeter (*x*-axis) versus average cluster area in square micrometer (*y*-axis) per condition. Ellipses represent 2D-SEM. Cells on Fn + β-glucan (blue) have a significant increase in both cluster number and area versus cell on Fn alone (red). Cells on Fn + β-glucan pretreated with VLA5 blocking mAb (pink) or VLA6 blocking mAb (purple) showed no significant difference in clustering parameters versus Fn + β-glucan (blue). Cells on Fn + β-glucan pretreated with VLA3 blocking mAb (black) or CR3 blocking mAb (green) a significant (*Figure legend continues*)

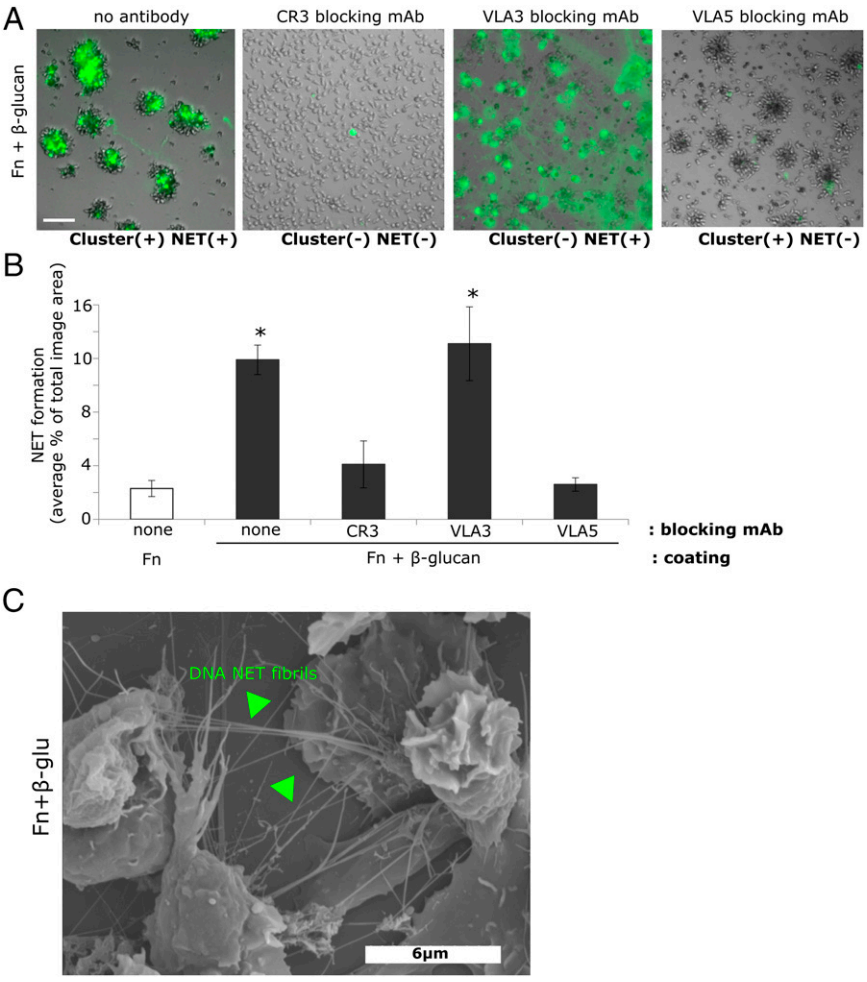

FIGURE 3. Neutrophil cluster formation and NETosis are regulated differentially by VLA3 and VLA5. (**A**) Human neutrophils assayed as in Fig. 2. After 30 min incubation, NET formation in the presence or absence of CR3, VLA3, or VLA5 blocking mAbs was visualized using Sytox green, imaged, and scored for NETs. Bright field and FITC images acquired at original magnification ×20; bar, 100 μm. (**B**) Quantification of NET formation. NETs were visualized with Sytox green and multiple images were taken per well. Images were thresholded and gated to include NETs and exclude nuclei. NET formation was quantified as a percentage area of the total imaged field. Well averages were ensemble averaged to generate this data. *$p < 0.001$ versus Fn alone, ANOVA full factorial, post hoc Newman–Keuls; error bars represent SEM. (**C**) Original magnification ×80, scanning electron microscopy images of neutrophils demonstrating NET elaboration. Neutrophils were prepared as described above, adhered to Fn + β-glucan coated wells for 30 min at 37°C, then fixed and prepared for scanning electron microscopy. DNA NET fibrils spanning aggregated neutrophils indicated by arrowheads.

CR3-to-VLA3 cross-talk. The preservation of NET formation after CR3 agonist treatment here suggests that the VLA5 role in NETosis is independent of CR3-to-VLA5 cross-talk.

VLA3 blocking peptide inhibits cluster formation but not NETosis

To confirm the regulatory role of VLA3 in cluster formation suggested by our VLA3 Ab blocking experiments, neutrophils were pretreated with 25 μg/ml of a cyclic VLA3 blocking peptide, LXY1, identified for its ability to block binding of VLA3 to laminin and shown to block VLA3-mediated leukocyte elongation (30, 31). Cells treated with the VLA3 blocking peptide then adhered to Fn + β-glucan–coated surfaces for 30 min at 37°C showed no significant change in NET formation when compared with untreated cells (Fig. 6A, 6B), but showed a complete abrogation of cluster formation (Figs. 5C, 6A). These data confirm Ab blocking data in supporting both a regulatory role for VLA3 in cluster formation and the β_1-mediated decoupling of cluster formation and NETosis.

Activation of VLA3 is significantly increased by CR3 on Fn + β-glucan–coated surfaces

Total VLA3 surface expression in neutrophils after exposure to Fn + β-glucan was unaltered as determined by staining using a directly conjugated Ab to VLA3 (ASC-1) with an average MFI ratio of Fn to Fn + β-glucan of 1.08 ± 0.13 (Fig. 7A). To determine if CR3 activation in turn caused activation of VLA3, we needed to develop an assay for VLA3 activation as there are no commercially available Abs that bind a VLA3 activation-specific epitope. To quantify conformational changes in VLA3 induced by Fn + β-glucan, we adapted a fluorescence resonance energy transfer (FRET)-based headpiece extension assay previously described for CR3 (25, 26). This FACS-based assay reports the relative distance between a FITC-labeled mAb to an epitope on the integrin headpiece and ORB, a membrane-partitioning fluorophore. To measure the conformational change of VLA3, we used the anti-VLA3 Ab clone ASC-1, which has been shown to block VLA3 binding to laminin but not to Fn or collagen type IV (32). Use of ASC-1 in our cell aggregation assay confirmed that it had no blocking function

decrease in clustering parameters versus Fn + β-glucan (blue) to levels statistically indistinguishable from cells on Fn alone (red). $p < 0.001$, ANOVA full factorial, post hoc Newman–Keuls. (**C**) CR3 adhesion to Fn + β-glucan results in auto-activation of CR3 but no significant change in surface expression. Representative histograms of neutrophils assayed as described on Fn (red), Fn + β-glucan (blue) or Fn + β-glucan in the presence of CR3 blocking mAb (green). After 30 min incubation, neutrophils were isolated and stained with directly conjugated mAbs for both total CR3 (top panel) and a CR3 activation specific epitope (bottom panel) and assayed by FACS. (**D**) The bar graph shows the average ratio of the MFI for cells adhered to Fn + β-glucan versus Fn alone. Control conditions show no significant difference in staining for total CR3 (white bars) but a significant increase in CR3 activation specific epitope staining (gray bars) on Fn + β-glucan versus Fn alone. Ab blocking of VLA3 or VLA5 does not significantly influence the expression or activation of CR3 in response to Fn + β-glucan versus Fn alone. Error bars represent SD. *$p < 0.001$, Fn + β-glucan versus Fn alone.

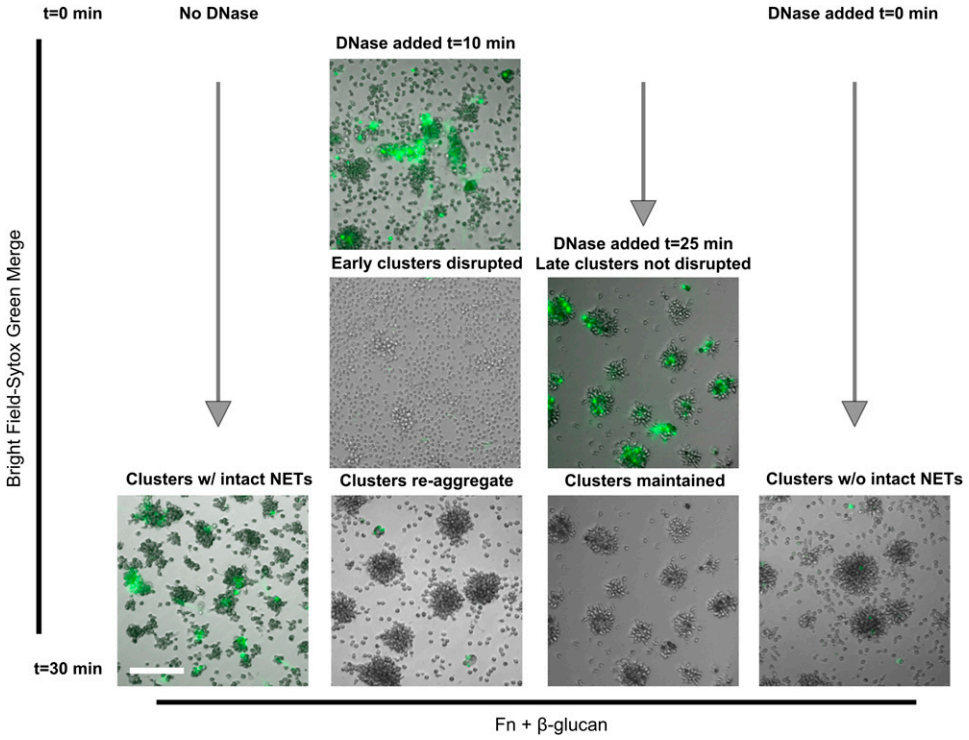

FIGURE 4. Dissolution of NETs by DNase I disrupts early, but not late, neutrophil clusters. Neutrophil clusters form in the absence of intact NET structures. Human neutrophils assayed as in Fig. 2 on Fn + β-glucan. DNase I was added either at time 0 before any neutrophil clusters had formed, after 10 min when early clusters had formed and associated NETs could be visualized, or after 25 min with matured clusters and associated NETs could be visualized. After 30 min incubation, cluster formation and NETs in the presence or absence of DNase I was visualized using Sytox green and imaged. Bright field and FITC images acquired at original magnification ×20; bar, 100 μm.

(Fig. 7B) with regard to clustering on Fn + β-glucan. Neutrophils assayed on Fn ± β-glucan–coated surfaces were isolated and stained with FITC-conjugated ASC-1 and aliquots were costained with increasing concentrations of ORB and assayed by FACS. Energy transfer from the FITC donor to the ORB acceptor causes a decrease in FITC intensity (quenching) that is proportional to the distance between the donor and acceptor fluorophores. The degree of this quenching gives a readout of VLA3 activity measured as headpiece extension (schematized in Fig. 7C). FACS data are analyzed by plotting the ratio of FITC MFI in the absence of ORB acceptor (F_d) to that in the presence of ORB acceptor (F_{da}) versus ORB mean fluorescence (Fig. 7D). The slope of these lines quantitatively represents the extent of energy transfer from the donor to the acceptor, with a steep slope reporting significant quenching of the FITC reporter Ab characteristic of an inactive receptor with its headpiece in close proximity to the cell membrane acceptor fluorophore and a shallow slope characteristic of an active receptor with its headpiece and associated FITC reporter Ab extended away from the cell membrane and unable to undergo FRET transfer to the cell membrane receptor (Fig. 7C, 7D).

Using FITC-ASC-1, we found a decreased slope reported for neutrophils adhered on Fn+β-glucan than reported for neutrophils adhered on Fn alone for 30 min at 37˚C and an average distance ratio of 1.67 ± 0.13, indicating that VLA3 is activated on Fn + β-glucan (Fig. 7D). This VLA3 activation is significantly reduced to an average distance ratio of 1.31 ± 0.05 when neutrophils are pretreated with a CR3 blocking mAb (44abc) providing evidence for a CR3-to-VLA3 cross-talk mechanism that drives neutrophil aggregation to Fn + β-glucan (Fig. 7D).

Activation of VLA5 is significantly decreased by CR3 on Fn + β-glucan and is required to permit VLA3 cluster formation

We determined if there was differential expression or activation of VLA5 on Fn + β-glucan versus on Fn alone during NETosis. FACS analysis using a directly conjugated mAb to total VLA5 (P1D6) showed no significant change in VLA5 expression over the conditions tested (Fig. 8A, left panel). However, staining with an activation-specific epitope of VLA5 (SNAKA51) suggested neutrophils that were adhered on Fn + β-glucan surfaces for 30 min at 37˚C had significantly less activated VLA5 than those adhered to surfaces coated with Fn alone and this decrease in activity was seen in neutrophils pretreated with an CR3 blocking mAb (Fig. 8A, right panel).

Findings in Fig. 3A show that VLA5 blocking does not impede neutrophil clustering on Fn + β-glucan and Fig. 8A indicates that VLA5 undergoes a suppression of the high affinity state prior to clustering. To determine if reduced activation of VLA5 is required for neutrophil cluster formation, we took advantage of a VLA5 activating mAb (SNAKA51) that binds an epitope mapped to the calf-1/calf-2 domains of the α_5 subunit and drives VLA5 into a high affinity state (33). Neutrophils pretreated with the VLA5-activating mAb and adhered to Fn + β-glucan–coated surfaces for 30 min at 37˚C showed no significant difference in NETosis when compared with control cells (Fig. 8B, 8C) but had a complete abrogation of neutrophil cluster formation (Fig. 8B, 8D). This suggests that VLA5 must be actively inhibited to allow for neutrophil aggregation in response to Fn + β-glucan.

Driving VLA5 activation does not affect CR3 expression or activation

We determined CR3 activity in neutrophils that had been pretreated with the VLA5 activating mAb (SNAKA51) and adhered to Fn + β-glucan for 30 min at 37˚C. By staining neutrophils with directly conjugated mAbs reporting both CR3 expression (ICRF44) and CR3 activation (CBRM1/5), we found that driving activation of VLA5 had no significant effect on CR3 expression or activation status (Fig. 9A), indicating that activating VLA5 blocks aggregate formation in a CR3 independent mechanism and provides additional evidence against a mechanism of β_1-to-β_2 cross-talk in this system.

To determine if there was a VLA5-to-VLA3 mechanism of VLA3 activation, we examined the activation state of VLA3 using the VLA3 ORB-FRET activation assay described previously (Fig. 7C, 7D). Neutrophils pretreated with VLA5 activating mAb (SNAKA51) for 30 min at 37˚C, were isolated and stained with a

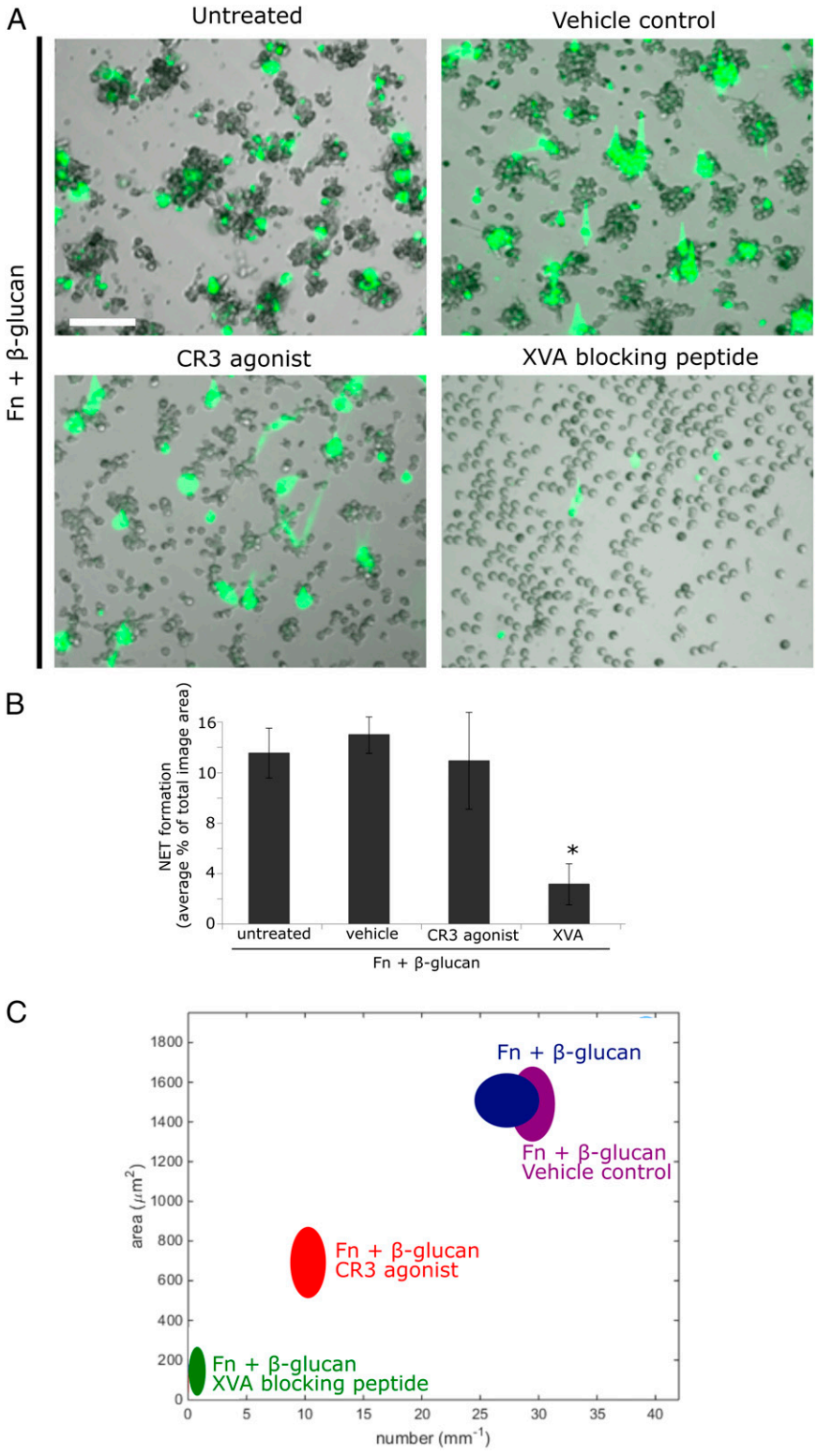

FIGURE 5. Leukadherin-1 allows NET formation but attenuates cluster formation. XVA143 blocks both cluster formation and NETosis. (**A**) Human neutrophils assayed as in Fig. 2. Where indicated, neutrophils were additionally pretreated either with CR3 agonist LA1, β_2 allosteric antagonist XVA, or vehicle control. After 30 min incubation, NET formation was visualized using Sytox green, imaged, and scored for NETs. Bright field and FITC images acquired at original magnification ×20; bar, 100 μm. (**B**) Quantification of NET formation. NETs were visualized with Sytox green and multiple images were taken per well. Images were thresholded and gated to include NETs and exclude nuclei. NET formation was quantified as a percentage area of the total imaged field. Well averages were ensemble averaged to generate this data. $*p <$ 0.001, XVA versus all other conditions, ANOVA full factorial, post hoc Newman–Keuls; error bars represent SEM. (**C**) Neutrophil cluster formation was quantified using ImageJ and custom MatLab software and plotted as average clusters per millimeter (*x*-axis) versus average cluster area in square micrometers (*y*-axis) per condition. Ellipses represent 2D-SEM. Cells on Fn + β-glucan pretreated with the XVA β_2 antagonist (green) have a significant decrease in both cluster number and area versus cells on Fn + β-glucan (blue). Cells on Fn + β-glucan pretreated with vehicle control (purple) showed no significant difference in clustering parameters versus Fn + β-glucan (blue). Cells on Fn + β-glucan pretreated with the CR3 agonist LA1 (red) showed an intermediate phenotype with a significant decrease in clustering parameters versus Fn + β-glucan (blue) but a significant increase in clustering parameters versus cells pretreated with the XVA blocking peptide (green). $p < 0.001$, ANOVA full factorial, post hoc Newman–Keuls.

directly conjugated mAb for a VLA3 (ASC-1), then aliquoted, incubated with increasing amounts of ORB, and analyzed by FACS. The ratio of FITC MFI in the absence of ORB acceptor (F_d) to that in the presence of ORB acceptor (F_{da}) versus ORB mean fluorescence was plotted (Fig. 9B). We observed no significant differences in slope or average distance ratios reported for neutrophils treated with VLA5 activating mAb (SNAKA51) adhered on Fn + β-glucan than reported for control neutrophils adhered on Fn+β-glucan (Fig. 9B), suggesting that any role of VLA5 in cluster formation is downstream of VLA3 and not a mechanism of VLA5-dependent activation of VLA3.

Behavior of human neutrophils in response to intact hyphae elaborated in the context of Fn show that NET formation and clustering can be decoupled in response to intact hyphae

To determine if the neutrophil integrin cross-talk response to Fn + β-glucan translates to the neutrophil response to intact hyphae in

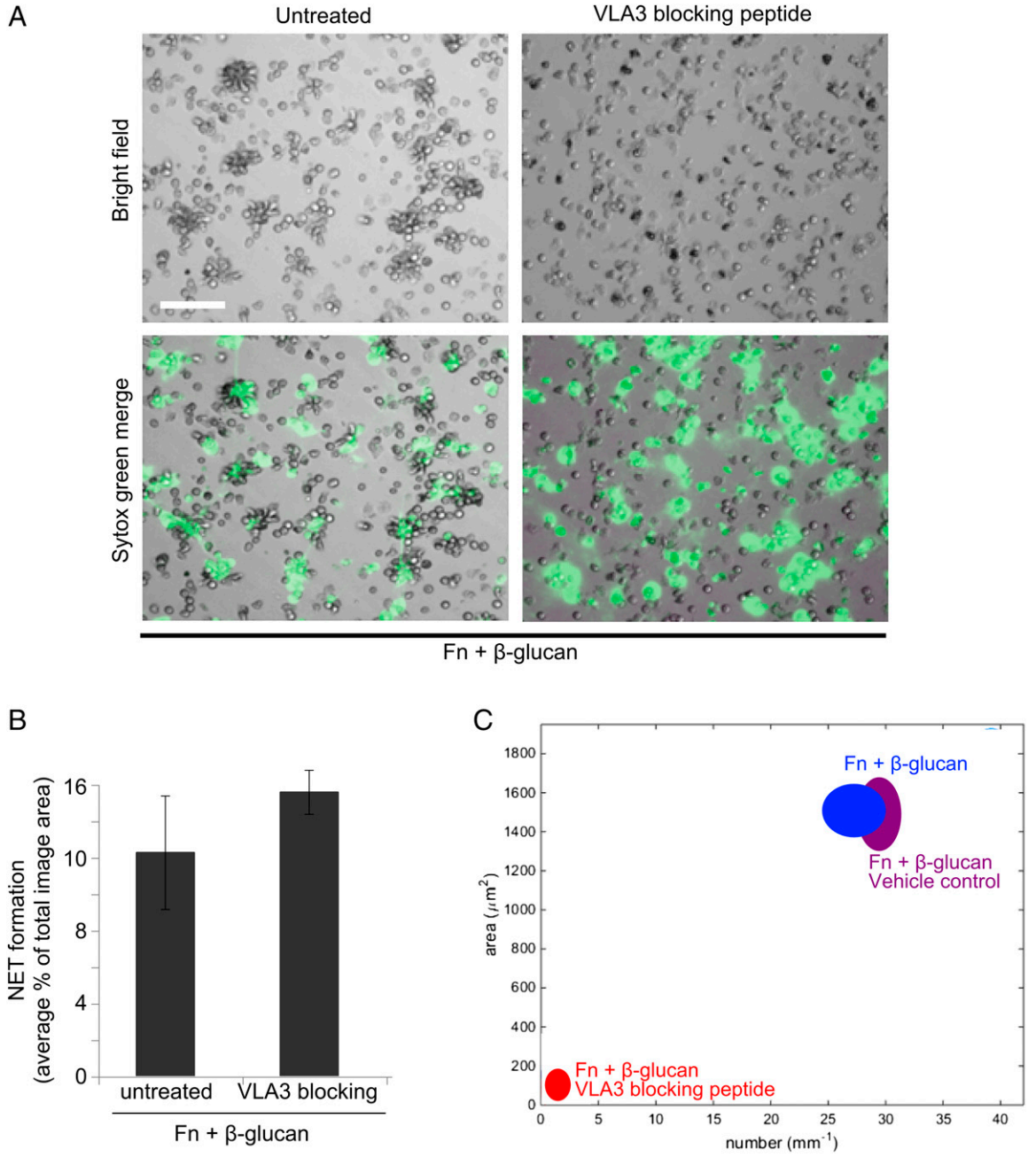

FIGURE 6. VLA3 blocking peptide, LXY1, blocks cluster formation but not NETosis. (**A**) Human neutrophils assayed as in Fig. 2 in the presence or absence of pretreatment with 25 μg/ml VLA3 blocking peptide LXY1. After 30 min incubation, NET formation was visualized using Sytox green, imaged, and scored for NETs. Bright field and FITC images acquired at original magnification ×20; bar, 100 μm. (**B**) Quantification of NET formation. NETs were visualized with Sytox green and multiple images were taken per well. Images were thresholded and gated to include NETs and exclude nuclei. NET formation was quantified as a percentage area of the total imaged field. Well averages were ensemble averaged to generate this data. Error bars represent SEM. (**C**) Quantification of cluster formation, which was done using custom MatLab software and plotted as average clusters per millimeter (*x*-axis) versus average cluster area in square micrometers (*y*-axis) per condition. Ellipses represent 2D-SEM. Cells on Fn + β-glucan pretreated with the LXY1 VLA3 blocking peptide (red) have a significant decrease in both cluster number and area versus cells on Fn + β-glucan (blue). Cells on Fn + β-glucan pretreated with vehicle control (purple) showed no significant difference in clustering parameters versus Fn + β-glucan (blue). $p < 0.001$, ANOVA full factorial, post hoc Newman–Keuls.

the context of matrix, we elaborated *C. albicans* hyphae on tissue culture, plastic coated with 10 μg/ml Fn at 37°C as previously described (19). Hyphae were washed and human neutrophils, pretreated on ice with 10^{-9} M fMLP, were added and incubated at 37°C in L-15 supplemented with 2 mg/ml glucose and 1 mM Mn^{++}. Where indicated, neutrophils were additionally pretreated either with specific mAbs to block VLA5 (P1D6) or VLA3 (M-KID2) or to activate VLA5 (SNAKA51). After 30 min at 37°C, NET formation was visualized using Sytox green (Fig. 10). Consistent with the neutrophil response to Fn + β-glucan, neutrophils clustered around hyphal filaments and elaborated NETs (Fig. 10A, 10C). Also consistent with findings using immobilized β-glucan, blocking VLA5 inhibited NETs but not clustering, and blocking VLA3 inhibited clustering but not NETs (Fig. 10B, 10C). Additionally, activation of VLA5 blocked clustering but not NETs (Fig. 10B, 10C). These data show that neutrophil NET formation

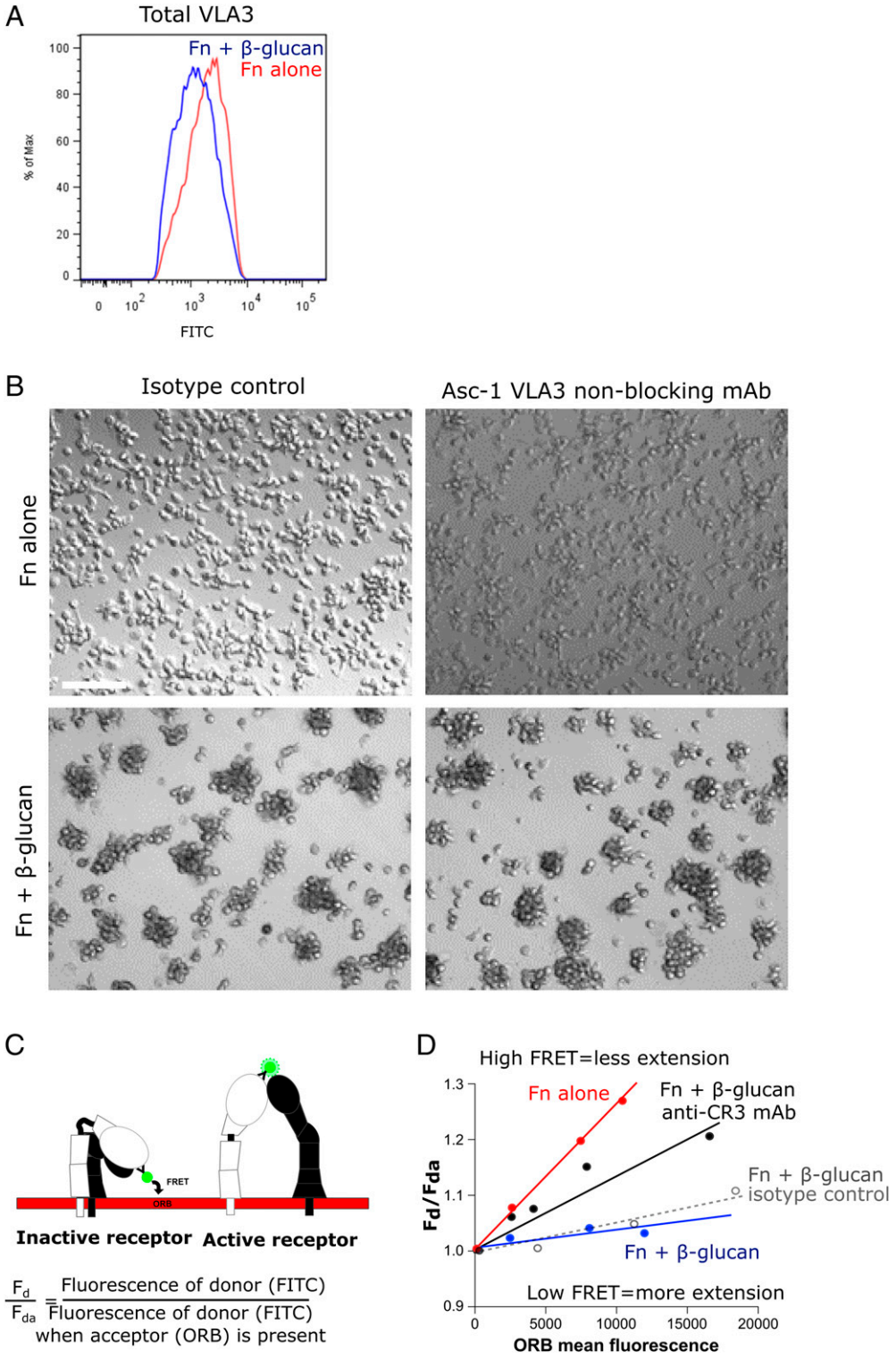

FIGURE 7. VLA3 activation is significantly increased on Fn + β-glucan versus Fn-coated surfaces and is mediated by CR3. (**A**) Human neutrophils assayed as in Fig. 2. After 30 min incubation, neutrophils were isolated and stained with a directly conjugated mAb for a VLA3. FACS histogram showing total VLA3 on Fn (red) and Fn + β-glucan (blue). (**B**) Human neutrophils assayed as in Fig. 2 in the presence of the non-function blocking VLA3 mAb ASC-1 or isotype control. After 30 min incubation, bright field images acquired at original magnification ×20; bar, 100 μm. (**C**) Shown is a schematic demonstrating the loss of FRET between ORB membrane dye and FITC-conjugated VLA3 mAb upon the extension of the extracellular domain. (**D**) Human neutrophils assayed as in Fig. 2 in the presence or absence of CR3 blocking mAb (44abc) or isotype control. After 30 min incubation, neutrophils were isolated and stained with a directly conjugated mAb for a VLA3 (Asc-1). Neutrophils were then incubated with 0, 75, 200, or 400 nM ORB and then analyzed by FACS. Representative data are plotted as the fraction of donor mean fluorescence intensity in the absence of acceptor fluorophore (F_d) to that in the presence of acceptor fluorophore (F_{da}) on the *y*-axis (F_d/F_{da}) versus ORB mean fluorescence on the *x*-axis.

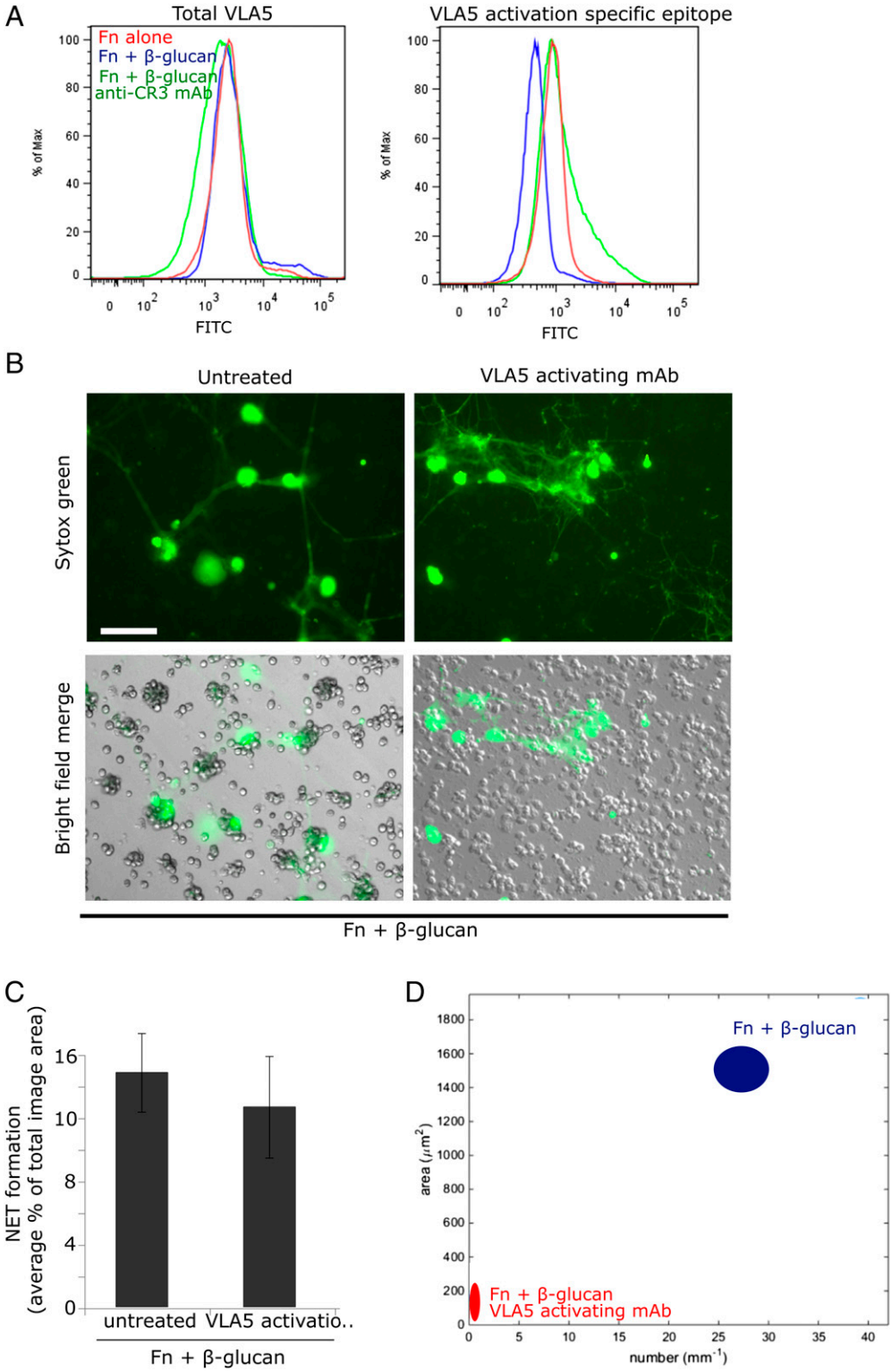

FIGURE 8. VLA5 shows a CR3-dependent reduction in activity on Fn + β-glucan versus Fn-coated surfaces. Driving VLA5 activation with an activating mAb blocks cluster formation but not NETosis, suggesting that an active inhibition of VLA5 is required for cluster formation. (**A**) Human neutrophils assayed as in Fig. 2. After 30 min incubation, neutrophils were isolated and stained with a directly conjugated mAb for either total VLA5 (P1D6) or an activation specific epitope of VLA5 (SNAKA51). FACS histogram showing VLA5 staining of cells adhered to Fn (red), Fn + β-glucan (blue), or Fn + β-glucan after pretreatment with a CR3-blocking mAb (green). (**B**) Human neutrophils assayed as above in the presence or absence of pretreatment with VLA5 activating mAb. After 30 min incubation, NET formation was visualized using Sytox green, imaged, and scored for NETs. Bright field and FITC images acquired at original magnification ×20; bar, 100 μm. (**C**) Quantification of NET formation. NETs were visualized with Sytox green and multiple images were taken per well. Images were thresholded and gated to include NETs and exclude nuclei. NET formation was quantified as a percent area of the total imaged field. Well averages were ensemble averaged to generate this data. Error bars represent SEM. (**D**) Quantification of cluster formation. Cluster formation was quantified using custom MatLab software and plotted as average clusters per millimeter (*x*-axis) versus average cluster area in square micrometers (*y*-axis) per condition. Ellipses represent 2D-SEM. Cells on Fn + β-glucan pretreated with the VLA5 activating mAb (red) have a significant decrease in both cluster number and area versus cells on Fn + β-glucan (blue). $p < 0.001$, ANOVA full factorial, post hoc Newman–Keuls.

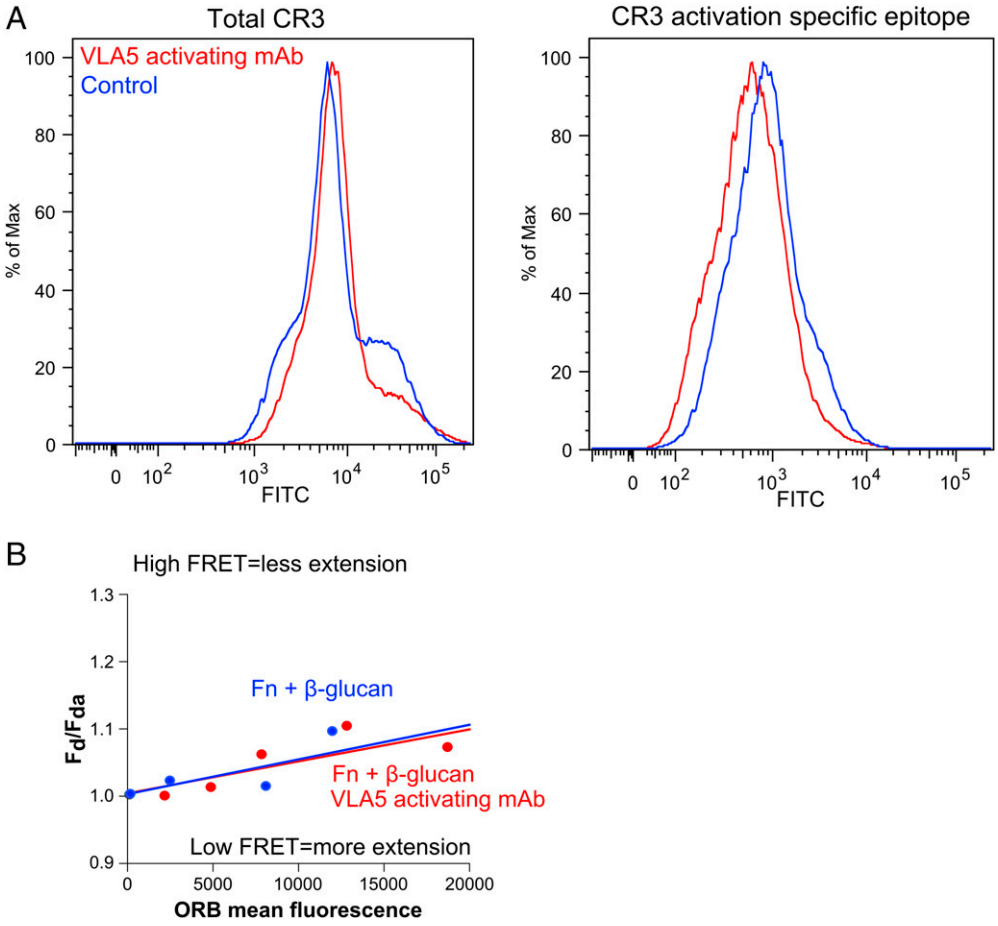

FIGURE 9. Driving VLA5 activation does not affect CR3 expression or activation, providing additional evidence dismissing β_1-to-β_2 cross-talk in this system. Additionally, driving VLA5 activation does not affect VLA3 activation, suggesting that VLA5's role in the regulation of cluster formation is downstream of CR3 and VLA3. Human neutrophils assayed as in Fig. 2 in the presence or absence of pretreatment with VLA5 activating mAb (SNAKA51). (**A**) After 30 min incubation, neutrophils were isolated and stained with directly conjugated mAbs for both total CR3 (ICRF44) and a CR3 activation specific epitope (CBRM1/5). FACS histograms showing total CR3 (left) and CR3 activation (right) on Fn and Fn + β-glucan for control cells (blue) and cells treated with the VLA5 activating mAb (red). (**B**) After 30 min incubation, neutrophils were isolated and stained with a directly conjugated mAb for a VLA3 (ASC-1). Neutrophils were then incubated with 0, 75, 200, or 400 nM ORB and analyzed by FACS. Representative data are plotted as the fraction of donor MFI in the absence of acceptor fluorophore (F_d) to that in the presence of acceptor fluorophore (F_{da}) on the *y*-axis (F_d/F_{da}) versus ORB mean fluorescence on the *x*-axis.

and clustering can be decoupled in response to intact hyphae as found for immobilized β-glucan.

A time course analysis of integrin activation in neutrophils adhered to Fn ± β-glucan supports a temporal model of integrin cross-talk

We reported that the neutrophil response to Fn + β-glucan NET formation occurs very rapidly, with cells undergoing this rapid NETosis serving as foci for neutrophil cluster formation. To extend these data presented to the current study, we undertook a time course analysis of integrin activation in neutrophils adhered to Fn ± β-glucan. Human neutrophils assayed as described previously were isolated after 5, 15, and 30 min incubation, stained with directly conjugated mAbs for a CR3 activation specific epitope (CBRM1/5) or a VLA5 activation specific epitope (SNAKA51) and assayed by FACS. Neutrophils adhered to Fn + β-glucan showed a significant time-dependent increase in CR3 activation that was not seen in cells adhered to Fn alone (Fig. 11A). Cells adhered to Fn ± β-glucan both showed a significant increase in VLA5 activation between 5 and 15 min that was sustained through 30 min on Fn alone (Fig. 11B). Cells adhered to Fn + β-glucan then showed a significant reduction in VLA5 activation at 30 min when compared with 15 min (Fig. 11B, right panel). To examine VLA3 activation, after 5 and 30 min incubation on Fn ± β-glucan, neutrophils were isolated and stained with a directly conjugated mAb for VLA3 (ASC-1). Neutrophils were then incubated with 0, 75, 200, or 400 nM ORB and then analyzed by FACS. Representative data are plotted as the fraction of donor mean fluorescence intensity in the absence of acceptor fluorophore (F_d) to that in the presence of acceptor fluorophore (F_{da}) on the *y*-axis (F_d/F_{da}) versus ORB mean fluorescence on the *x*-axis. Quenching of the VLA3 reporter mAb of neutrophils adhered to Fn alone had a steep slope indicating low activity at 5 min (data not shown) that was maintained through 30 min with no significant difference in average distance ratios (Fig. 11C). Cells adhered to Fn + β-glucan, however, had a steep slope not significantly different from that of cells on Fn alone at 5 min indicating low activity, but a significantly shallower slope at 30 min indicating increased VLA3 activity with an average distance ratio of 1.53 ± 0.13. These data suggest that integrin regulation in response to Fn + β-glucan is a temporally coordinated process (Fig. 12).

Discussion

Systemic infection caused by *Candida* species is the fourth leading cause of nosocomial bloodstream infection in modern hospitals

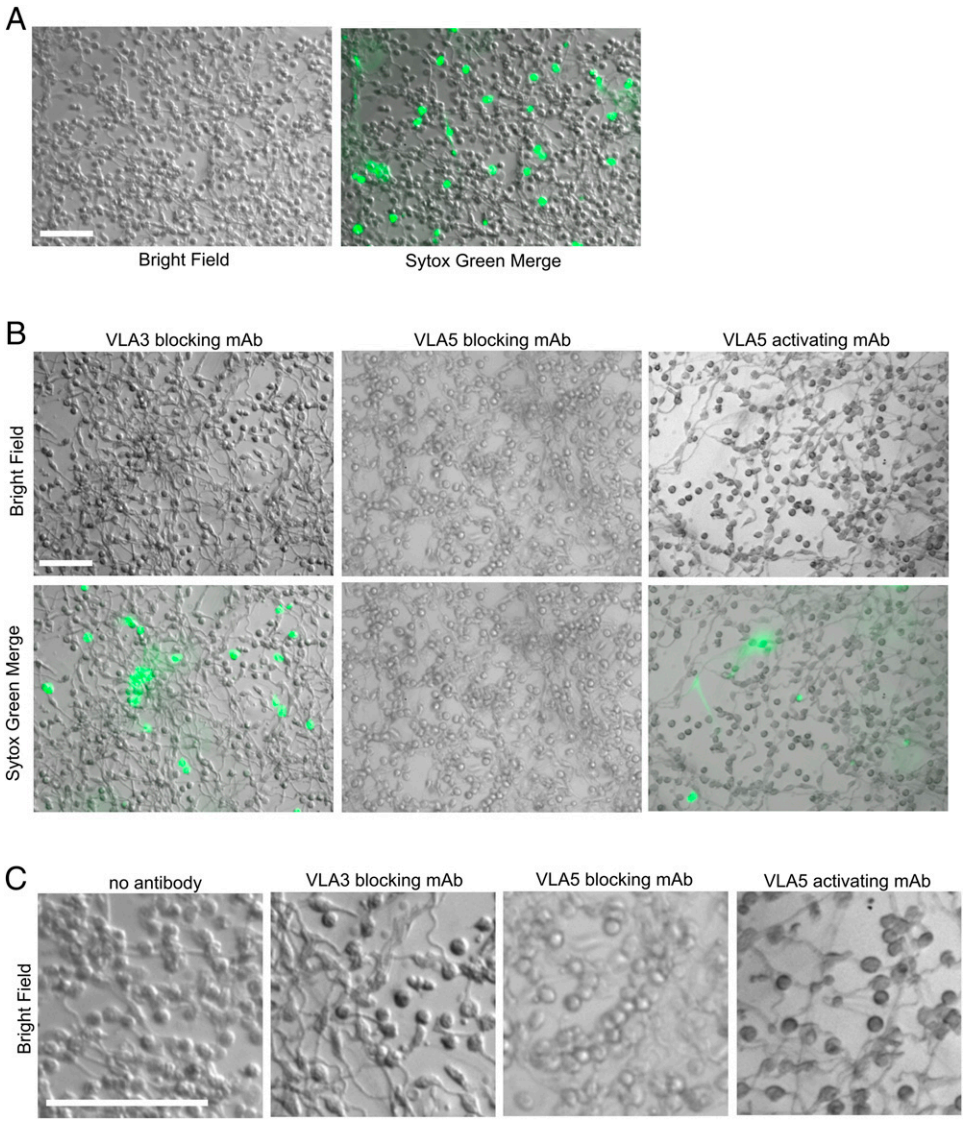

FIGURE 10. Behavior of human neutrophils in response to intact hyphae elaborated in the context of Fn show that NET formation and clustering can be decoupled in response to intact hyphae. *C. albicans* blastoconidia were allowed to elaborate into hyphae on tissue culture plastic coated with 10 μg/ml Fn in YPD at 37°C. Hyphae were washed and human neutrophils, pretreated on ice with 10^{-9} M fMLP, were added and incubated at 37°C in L-15 supplemented with 2 mg/ml glucose and 1 mM Mn^{++}. After 30 min incubation, NET formation was visualized using Sytox green, imaged, and scored for cluster formation and NETs with (**A**) control cells and (**B**) neutrophils that were additionally pretreated either with specific mAbs to block VLA5 (P1D6) or VLA3 (MKID-2) or to activate VLA5 (SNAKA51). Bright field and FITC images acquired at original magnification ×20; bar, 100 μm. (**C**) Enlarged images showing cluster aggregation to hyphae.

and carries high morbidity and mortality rates despite antifungal therapy. In the last three decades, there has been an increase in fungal infections in patients who are immunosuppressed or neutropenic (1, 7). Current studies of fungal infection trends show resistance is increasing among fungal species susceptible to these drugs (34, 35). To combat rising fungal infection rates and growing resistance, an increased focus on additional ways to enhance the innate immune antifungal response may offer alternative treatments.

Neutrophils are the primary cells responsible for the elimination of fungi in invasive tissue infections, yet the mechanisms by which they respond to virulence-associated, non-ingestible hyphal forms of fungi are poorly understood. The aim of this study was to investigate the surface receptors involved in the neutrophil response to fungal β-glucan in the context of the ECM protein, Fn. This is motivated by the widespread tissue distribution of Fn and the contact with this matrix component by neutrophils responding to deep-seated mycosis. Prior work from our laboratory showed that neutrophil swarming and clustering as well as NET release to β-glucan and intact hyphae are dependent on Fn. The swarming of neutrophils and eventual clustering around hyphal filaments, along with NET release, are regarded as essential components for effective host defense against this dimorphic opportunist. In pursuit of a better understanding of this matrix-dependent immune response, we now demonstrate a novel, complex, and temporally regulated cross-talk pathway in which the β_2 integrin CR3 signals the differential regulation of individual β_1 integrins not often associated with antifungal activity. We show that NETosis and swarming/clustering are controlled by the activation state of distinct β_1 integrins, with both effects ultimately regulated by CR3. Our data support a two-stage temporal model (schematized in Fig. 12) where VLA5 and CR3 are activated by ligand binding immediately following contact with Fn and β-glucan leading to rapid, matrix-dependent NET formation. Over time, CR3 undergoes inside-out auto-activation that drives the downregulation (suppression) of VLA5 and the upregulation (activation) of VLA3 to allow for swarming/cluster formation (Fig. 11). If VLA5 is not downregulated, clustering is obviated. This study not only reinforces the need to account for the matrix to fully understand mechanisms of antifungal host defense, but also reveals new roles for β_1 integrins in host defense to *Candida*. We also show a previously unappreciated level of complexity and interfamily communication among β_1 and β_2 integrins.

A significant finding of this paper is the ability of CR3 to coordinate a simultaneous upregulation and downregulation of two distinct β_1 integrins in response to fungi via integrin cross-talk. Integrin cross-talk was first described as *trans*-dominant inhibition in which activation of one integrin prevented the activity of

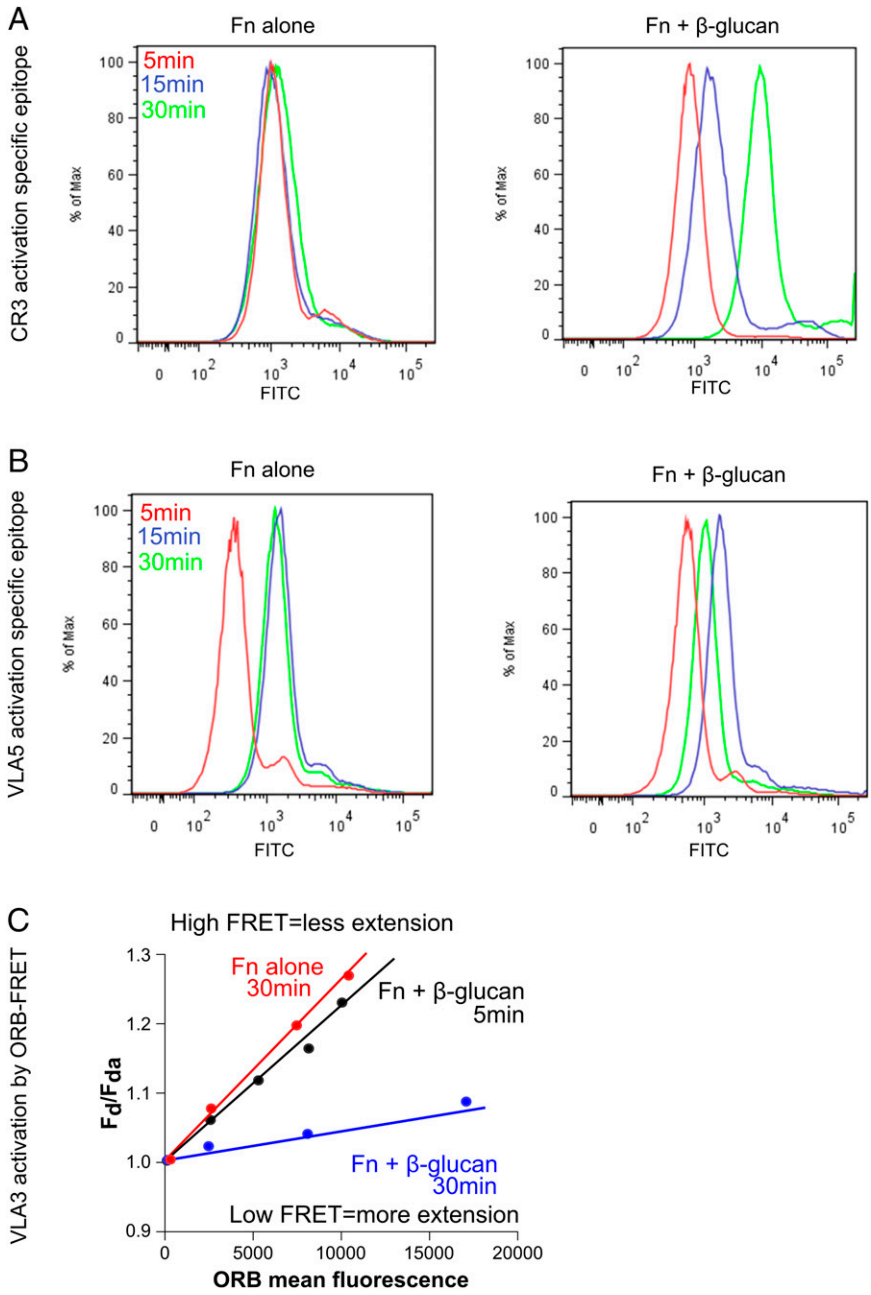

FIGURE 11. A time course analysis of integrin activation in neutrophils adhered to Fn + β-glucan supports temporal model of regulation. Human neutrophils assayed as in Fig. 2A were pretreated on ice with 10^{-9} M fMLP, incubated at 37°C on tissue culture plastic coated with either Fn alone or six Fn + β-glucan in L-15 supplemented with 2 mg/ml glucose and 1 mM Mn^{++}. After 5, 15, and 30 min incubation, cells were isolated and stained with directly conjugated mAbs for a CR3 activation specific epitope (CBRM1/5) or a VLA5 activation specific epitope (SNAKA51) and assayed by FACS. FACS histograms showing CR3 activation (**A**) and VLA5 activation (**B**) for cells adhered to Fn alone (left panel) and Fn + β-glucan (right panel) for 5 min (red), 15 min (blue), or 30 min (green). (**C**) Neutrophils assayed as described above. After 5 and 30 min incubation, neutrophils were isolated and stained with a directly conjugated mAb for VLA3 (ASC-1). Neutrophils were then incubated with 0, 75, 200, or 400 nM ORB and then analyzed by FACS. Representative data are plotted as the fraction of donor mean fluorescence intensity in the absence of acceptor fluorophore (F_d) to that in the presence of acceptor fluorophore (F_{da}) on the *y*-axis (F_d/F_{da}) versus ORB mean fluorescence on the *x*-axis.

another integrin through intracellular signaling and has since evolved to encompass many types of inter-integrin regulation (36, 37). For example, on T cells, the β_2 integrin LFA-1 downregulates the VLA4 response to ECM while upregulating the VLA5 response to Fn to allow for stronger adhesion (38). Our findings offer new insight into the molecular mechanisms underlying the neutrophil response to fungal β-glucan in the context of the tissue matrix. We propose CR3 as the master regulator,

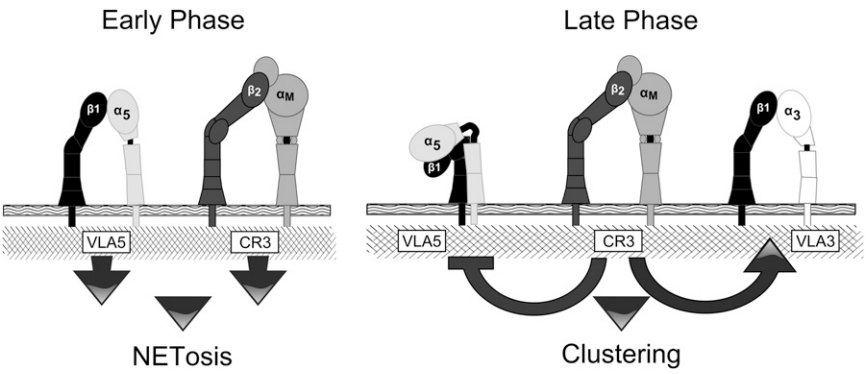

FIGURE 12. Two-stage model of integrin cross-talk in mediating neutrophil clustering and NETosis on Fn + β-glucan that decouples clustering and NET formation. We propose an early stage of VLA5 and CR3 adhesion to Fn + β-glucan that triggers NETosis and subsequent CR3 inside-out auto activation that leads to a later stage β_2-to-β_1 cross-talk that inactivates VLA5 and activates VLA3 leading to characteristic neutrophil clustering around NETotic foci.

coordinating the *trans*-dominant inhibition of VLA5 and the up-regulation of VLA3, resulting in neutrophil swarming and homotypic aggregation.

Our initial observation of neutrophils swarming into clusters on immobilized Fn and β-glucan or hyphae led us to question the importance of cluster formation in the immune response to fungi. Others have suggested that as hyphal forms of fungi are much too large to be phagocytosed, neutrophils circumvent this problem by enclosing microbes together with other neutrophils (39, 40). The encompassment of the microbe may provide areas of concentrated neutrophilic effector activity better able to eliminate the infection than would occur by binding single cells along a hyphal filament (18). We identify VLA3 activity as necessary for clustering. This is consistent with previous work in our laboratory, which has shown that upon dual ligation of CR3 by Fn and β-glucan, neutrophils demonstrated enhanced chemotaxis mediated by a shift in Fn binding from VLA5 to VLA3 (41).

However, we also consider an alternative to the essentiality of VLA3 activity and swarming to the antifungal response. It is plausible that the early NETotic response is responsible for hyphal killing and perhaps physical containment of blastoconidia, which serves to wall off the infectious focus. In addition to NETosis, some early-responding neutrophils likely elaborate chemokines (i.e., IL-8, LTB4) to attract the next wave of neutrophils into organized clusters with the initiating cell located centrally. It is not yet clear if NETosis and chemokine release results from the same cell or from neighboring early responders. Importantly, whether swarming is essential or dispensable to host defense remains to be confirmed. We recognize that VLA3-induced clustering could be a detrimental aspect of the inflammatory response and contribute to collateral tissue damage as a result of gathering a high concentration of neutrophils into a focal point. This allows for the hypothesis that, by targeting VLA3 activity, collateral tissue damage may be attenuated while maintaining the biologically important immune defense mechanism of NETosis. In support, it has been shown that VLA3-high expressing cells from septic animals displayed hyper-inflammatory phenotypes that when blocked or conditionally knocked down showed reduced extravasation and increased survival rates compared with healthy animals (42). Future work will test the host response of mice lacking VLA3 upon fungal challenge.

The role of VLA5 in matrix-dependent rapid NET formation has not been previously described. Whereas CR3 cross-talk affecting the affinity states of VLA3 and VLA5 is necessary for swarming and aggregation, whether cross-talk between CR3 and VLA5 regulates NETosis is less evident. Ab blocking of CR3 or VLA5 clearly prevents NETosis, suggesting a non-redundant role for these receptors in initiating NET release. The reason NET release on Fn + β-glucan necessitates binding of both receptors is not yet known. The requirement for CR3 was further supported by the β_2 integrin allosteric antagonist XVA143. The mechanism of action of CR3 small molecule agonist LA1, locking activated CR3 receptor into its structurally high affinity state while decoupling it from some of its intracellular communication within the cell, generated a slightly different result, affecting clustering more profoundly than NETosis for reasons yet to be discerned. That NET accumulation persisted over the 30 min observation period, even as VLA5 was becoming downregulated, suggests that NET triggering requires VLA5 activation but perhaps persistence of formation and release of NETs becomes constitutive after an initialization event. Of course, this scenario is difficult to discern at the population level and would necessitate determining the activation status of each NETotic cell to formally determine if a VLA5 high–affinity state is only needed initially to trigger NET release. By identifying VLA5 as having a role in NET formation, we have uncovered a new pharmaceutical molecular target for diseases exhibiting excessive NET formation while showing that different structural conformations of CR3 may mediate different cellular functions. Our results are also consistent with the reported finding that post-NETotic, anuclear neutrophils are capable of chemotaxis and bacterial phagocytosis perhaps representative of multitasking antimicrobial effector functions against fungal filaments (43). These authors concluded that NETosis is not limited to immobile and incapacitated cells and this may serve to aid the spread of microbiocidal NETs around the area surrounding a focus of infection to an extent greater than would be possible if NETosis was limited to nonmigratory neutrophils.

VLA5 binds Fn with high affinity at two locations: its RGD sequence, an Arg-Gly-Asp motif contained by many ECM proteins, and its PHSRN site, a Pro–His–Ser–Arg–Asn synergy sequence specific to Fn (44). Specifically, residue Asp154 distinguishes α_5 from other α subunits and results in its strong preference for Fn over other RGD ligands (45). VLA5 is unique in that the integrin conformation and the ligand binding are not mutually related. A recent study showed RGD-bound VLA5 structure conformation was similar to the non-ligated structure conformation. Furthermore, when bound with an inhibitor mAb, VLA5 was able to bind ligand (45). Taken together, this indicates VLA5 can bind Fn in what is considered the inactive confirmation. As inhibition of VLA5 extension does not necessarily mean it is unable to recognize ligand and communicate with the cell, perhaps a ligated VLA5 in a low-affinity conformation induces intracellular signaling not possible in its high-affinity state. Furthermore, Ab blockade of VLA5 receptor has no effect on the neutrophil response to Fn + β-glucan, indicating the addition of β-glucan inhibits the activity of VLA5 toward its canonical ligand Fn. The switch from VLA5 to VLA3 Fn affinity may facilitate a type of cellular migration that is not possible with the strong adhesion between VLA5 and Fn.

The recognition of immobilized β-glucan in the context of Fn shifts CR3 to a more activated state as determined by FACS using a CR3 activation reporter Ab (Fig. 2C). This activity is critical, as treatment with a CR3 blocking mAb (44abc) not only decreases CR3 activation, as measured by staining of a CR3 activation specific epitope (Fig. 2C), but also decreases the neutrophil response of swarming (Fig. 2A) and NET release (Fig. 3A, 3B). Additionally, we show with the use of a CR3 receptor agonist that locks activated CR3 into an extended conformation and decouples intracellular signaling, that CR3 must be able to move between its physical conformational states to allow for swarming (Fig. 5A). We demonstrate that CR3 and VLA3 activity, but not expression, is increased in the presence of β-glucan (Figs. 2C, 7A, 7D). In addition, VLA5 activity must be downregulated to allow for cluster formation (Fig. 8). This is because of the reduction in binding of the activation reporter Ab SNAKA51 observed on cells exposed to Fn + glucan, whereas no such reduction in total VLA5 expression is noted by the anti-VLA5 Ab P1D6, which binds to all VLA5 molecules regardless of activation state. Both SNAKA51 and P1D6 are well characterized to bind to VLA5 at epitopes that map outside the ligand-binding domain so expression of total and activated VLA5 receptors can be measured without interference by the presence of ligand. Taken together, CR3 serves as the master regulator of a full-blown neutrophilic response to fungal β-glucan in the context of matrix under conditions where phagocytosis is not available in host defense.

Previous work in our laboratory has suggested that dual ligation of CR3 affects β_1 subfamily integrins, VLA5 and VLA3, and can have effects on CR3–mediated antifungal responses via integrin

cross-talk. Harler et al. (41) showed migration on a Fn substrate was mediated by the integrins VLA5 and CR3; however, supplementation of the Fn with β-glucan led to a shift in integrin-mediated chemotaxis to one that is determined by VLA3. VLA3 contains binding domains for both laminin and RGD and it is this later functionality that controls migration on glucan when VLA5 is blocked. In addition, Lavigne et al. (46) proved blocking VLA5 or VLA3 was sufficient to relieve the Fn-dependent suppression of respiratory burst induced by the β-glucan activation of CR3. In the current study, we demonstrate CR3 participates in β_2-to-β_1 cross-talk with both VLA5 and VLA3 to determine the neutrophil response to either immobilized β-glucan or fungal hyphae in the context of Fn. We further show that β_1 integrins differentially regulate neutrophil function with VLA3 driving clustering and VLA5 being required for NETosis. Our body of work shows the essential role of matrix-to-integrin interactions in mediating the multiple neutrophil antifungal effector functions including chemotaxis, oxidative burst, clustering and NETosis. All these functions are initiated upon ligation of CR3 at the I-domain by fibronectin and at the lectin-like site by fungal β-glucan, and fully executed upon proper temporal regulation of the activation state of VLA3 and VLA5.

Our experiments demonstrate the mechanisms that form the early events leading to the antifungal response by neutrophils, which includes aggregation into an attack complex around a fungal hypha. Upon multifocal contact with matrix and fungal hyphae (or β-glucan), the earliest responding neutrophils undergo NETosis followed by aggregation. Our findings show that these NETotic neutrophils represent a minor population of the assayed cells; most cells are not associated with NET release. We presume these NETotic cells release an as yet undefined chemoattractant to which other polymorphonuclear leukocytes respond and gather as a subsequent wave of chemotactic neutrophils. This does not in any way preclude neutrophils that enter clusters later from releasing NETs, and in previous work we have shown that NETs released by neutrophils in our system are indeed cytotoxic for *Candida* hyphae (19). One may speculate that there is benefit to the host to have neutrophils perform multiple antimicrobial events in defense including NETosis to allow containment and clearance of a complex infection involving both yeast and hyphal forms in vivo. Consistent with this notion, we define the integrin-based mechanism that controls the early events leading to an amplification of a neutrophil-based cluster response that is likely to be a more efficient antifungal response than neutrophils responding individually.

Ultimately, this report provides insights on a newly recognized pathway of integrin cross-talk between the β_2 integrin CR3 and the β_1 integrins VLA3 and VLA5, and its role in the neutrophilic responses to fungal β-glucan. Whereas our current experimental focus is on the response to fungi, integrin cross-talk future work can be proposed to determine whether this is a universal component of the neutrophilic response to all microbial infections of tissues. These results may find new pathways to identify novel targets for antifungal therapy and immune cell enhancement as well as increase our understanding of the complex regulation of integrins. Target outcomes may provide an adjuvant or alternative therapy to combat the increasing fungal resistance to azole therapy and improve recovery time of patients with fungal infections.

Acknowledgments

We thank Dr. Meredith Crane and Allan Huang for technical assistance, Matthew Hirakawa and the Brown University Leduc Bioimaging Facility for SEM, and Kevin Carlson and the Brown University Flow Cytometry Facility for FACS acquisition.

Disclosures

J.S.R. is a shareholder in Biothera (Eagan, MN) and reports the gift of Imprime-PGG glucan for use in current studies from Biothera (Eagan, MN). V.G. is an inventor on pending patent applications and is also a cofounder of Adhaere Pharmaceuticals, Inc. (Skokie, IL) that has licensed these applications related to Leukadherin-1. V.G. has the potential for financial benefit from the future commercialization of these applications. The other authors have no financial conflicts of interest.

References

1. Wisplinghoff, H., T. Bischoff, S. M. Tallent, H. Seifert, R. P. Wenzel, and M. B. Edmond. 2004. Nosocomial bloodstream infections in US hospitals: analysis of 24,179 cases from a prospective nationwide surveillance study. *Clin. Infect. Dis.* 39: 309–317.
2. Marr, K. A., R. A. Carter, F. Crippa, A. Wald, and L. Corey. 2002. Epidemiology and outcome of mould infections in hematopoietic stem cell transplant recipients. *Clin. Infect. Dis.* 34: 909–917.
3. Horn, D. L., D. Neofytos, E. J. Anaissie, J. A. Fishman, W. J. Steinbach, A. J. Olyaei, K. A. Marr, M. A. Pfaller, C. H. Chang, and K. M. Webster. 2009. Epidemiology and outcomes of candidemia in 2019 patients: data from the prospective antifungal therapy alliance registry. *Clin. Infect. Dis.* 48: 1695–1703.
4. Zaoutis, T. E., J. Argon, J. Chu, J. A. Berlin, T. J. Walsh, and C. Feudtner. 2005. The epidemiology and attributable outcomes of candidemia in adults and children hospitalized in the United States: a propensity analysis. *Clin. Infect. Dis.* 41: 1232–1239.
5. Miller, L. G., R. A. Hajjeh, and J. E. Edwards, Jr. 2001. Estimating the cost of nosocomial candidemia in the United States. *Clin. Infect. Dis.* 32: 1110.
6. Wilson, L. S., C. M. Reyes, M. Stolpman, J. Speckman, K. Allen, and J. Beney. 2002. The direct cost and incidence of systemic fungal infections. *Value Health* 5: 26–34.
7. Edmond, M. B., S. E. Wallace, D. K. McClish, M. A. Pfaller, R. N. Jones, and R. P. Wenzel. 1999. Nosocomial bloodstream infections in United States hospitals: a three-year analysis. *Clin. Infect. Dis.* 29: 239–244.
8. Blumberg, H. M., W. R. Jarvis, J. M. Soucie, J. E. Edwards, J. E. Patterson, M. A. Pfaller, M. S. Rangel-Frausto, M. G. Rinaldi, L. Saiman, R. T. Wiblin, and R. P. Wenzel, National Epidemiology of Mycoses Survey (NEMIS) Study Group, The National Epidemiology of Mycosis Survey. 2001. Risk factors for candidal bloodstream infections in surgical intensive care unit patients: the NEMIS prospective multicenter study. *Clin. Infect. Dis.* 33: 177–186.
9. León, C., S. Ruiz-Santana, P. Saavedra, B. Almirante, J. Nolla-Salas, F. Alvarez-Lerma, J. Garnacho-Montero, and M. A. León, EPCAN Study Group. 2006. A bedside scoring system ("Candida score") for early antifungal treatment in nonneutropenic critically ill patients with Candida colonization. *Crit. Care Med.* 34: 730–737.
10. Manolakaki, D., G. Velmahos, T. Kourkoumpetis, Y. Chang, H. B. Alam, M. M. De Moya, and E. Mylonakis. 2010. Candida infection and colonization among trauma patients. *Virulence* 1: 367–375.
11. Kourkoumpetis, T., D. Manolakaki, G. Velmahos, Y. Chang, H. B. Alam, M. M. De Moya, E. A. Sailhamer, and E. Mylonakis. 2010. Candida infection and colonization among non-trauma emergency surgery patients. *Virulence* 1: 359–366.
12. Pfaller, M. A. 1999. Molecular epidemiology in the care of patients. *Arch. Pathol. Lab. Med.* 123: 1007–1010.
13. Engelhardt, K. R., and B. Grimbacher. 2012. Mendelian traits causing susceptibility to mucocutaneous fungal infections in human subjects. *J. Allergy Clin. Immunol.* 129: 294–305, quiz 306–307.
14. Puel, A., S. Cypowyj, J. Bustamante, J. F. Wright, L. Liu, H. K. Lim, M. Migaud, L. Israel, M. Chrabieh, M. Audry, et al. 2011. Chronic mucocutaneous candidiasis in humans with inborn errors of interleukin-17 immunity. *Science* 332: 65–68.
15. Van't Wout, J. W., J. W. Van der Meer, M. Barza, and C. A. Dinarello. 1988. Protection of neutropenic mice from lethal *Candida albicans* infection by recombinant interleukin 1. *Eur. J. Immunol.* 18: 1143–1146.
16. van den Berg, J. M., E. van Koppen, A. Ahlin, B. H. Belohradsky, E. Bernatowska, L. Corbeel, T. Español, A. Fischer, M. Kurenko-Deptuch, R. Mouy, et al. 2009. Chronic granulomatous disease: the European experience. *PLoS One* 4: e5234.
17. Cheng, S. C., L. A. Joosten, B. J. Kullberg, and M. G. Netea. 2012. Interplay between *Candida albicans* and the mammalian innate host defense. *Infect. Immun.* 80: 1304–1313.
18. Branzk, N., A. Lubojemska, S. E. Hardison, Q. Wang, M. G. Gutierrez, G. D. Brown, and V. Papayannopoulos. 2014. Neutrophils sense microbe size and selectively release neutrophil extracellular traps in response to large pathogens. *Nat. Immunol.* 15: 1017–1025.
19. Byrd, A. S., X. M. O'Brien, C. M. Johnson, L. M. Lavigne, and J. S. Reichner. 2013. An extracellular matrix-based mechanism of rapid neutrophil extracellular trap formation in response to *Candida albicans*. *J. Immunol.* 190: 4136–4148.
20. Xia, Y., and G. D. Ross. 1999. Generation of recombinant fragments of CD11b expressing the functional beta-glucan-binding lectin site of CR3 (CD11b/CD18). *J. Immunol.* 162: 7285–7293.
21. Forsyth, C. B., E. F. Plow, and L. Zhang. 1998. Interaction of the fungal pathogen *Candida albicans* with integrin CD11b/CD18: recognition by the I domain is modulated by the lectin-like domain and the CD18 subunit. *J. Immunol.* 161: 6198–6205.

22. Diamond, M. S., J. Garcia-Aguilar, J. K. Bickford, A. L. Corbi, and T. A. Springer. 1993. The I domain is a major recognition site on the leukocyte integrin Mac-1 (CD11b/CD18) for four distinct adhesion ligands. *J. Cell Biol.* 120: 1031–1043.
23. Thornton, B. P., V. Větvicka, M. Pitman, R. C. Goldman, and G. D. Ross. 1996. Analysis of the sugar specificity and molecular location of the beta-glucan-binding lectin site of complement receptor type 3 (CD11b/CD18). *J. Immunol.* 156: 1235–1246.
24. Bose, N., A. S. Chan, F. Guerrero, C. M. Maristany, X. Qiu, R. M. Walsh, K. E. Ertelt, A. B. Jonas, K. B. Gorden, C. M. Dudney, et al. 2013. Binding of soluble yeast β-glucan to human neutrophils and monocytes is complement-dependent. *Front. Immunol.* 4: 230.
25. Lefort, C. T., Y. M. Hyun, J. B. Schultz, F. Y. Law, R. E. Waugh, P. A. Knauf, and M. Kim. 2009. Outside-in signal transmission by conformational changes in integrin Mac-1. *J. Immunol.* 183: 6460–6468.
26. O'Brien, X. M., K. E. Heflin, L. M. Lavigne, K. Yu, M. Kim, A. R. Salomon, and J. S. Reichner. 2012. Lectin site ligation of CR3 induces conformational changes and signaling. *J. Biol. Chem.* 287: 3337–3348.
27. Welzenbach, K., U. Hommel, and G. Weitz-Schmidt. 2002. Small molecule inhibitors induce conformational changes in the I domain and the I-like domain of lymphocyte function-associated antigen-1. Molecular insights into integrin inhibition. *J. Biol. Chem.* 277: 10590–10598.
28. Yang, W., C. V. Carman, M. Kim, A. Salas, M. Shimaoka, and T. A. Springer. 2006. A small molecule agonist of an integrin, alphaLbeta2. *J. Biol. Chem.* 281: 37904–37912.
29. Maiguel, D., M. H. Faridi, C. Wei, Y. Kuwano, K. M. Balla, D. Hernandez, C. J. Barth, G. Lugo, M. Donnelly, A. Nayer, et al. 2011. Small molecule-mediated activation of the integrin CD11b/CD18 reduces inflammatory disease. *Sci. Signal.* 4: ra57.
30. Hyun, Y. M., R. Sumagin, P. P. Sarangi, E. Lomakina, M. G. Overstreet, C. M. Baker, D. J. Fowell, R. E. Waugh, I. H. Sarelius, and M. Kim. 2012. Uropod elongation is a common final step in leukocyte extravasation through inflamed vessels. *J. Exp. Med.* 209: 1349–1362.
31. Yao, N., W. Xiao, X. Wang, J. Marik, S. H. Park, Y. Takada, and K. S. Lam. 2009. Discovery of targeting ligands for breast cancer cells using the one-bead one-compound combinatorial method. *J. Med. Chem.* 52: 126–133.
32. Pattaramalai, S., K. M. Skubitz, and A. P. Skubitz. 1996. A novel recognition site on laminin for the α 3 β 1 integrin. *Exp. Cell Res.* 222: 281–290.
33. Clark, K., R. Pankov, M. A. Travis, J. A. Askari, A. P. Mould, S. E. Craig, P. Newham, K. M. Yamada, and M. J. Humphries. 2005. A specific alpha5beta1-integrin conformation promotes directional integrin translocation and fibronectin matrix formation. *J. Cell Sci.* 118: 291–300.
34. Pfaller, M. A., L. Boyken, R. J. Hollis, S. A. Messer, S. Tendolkar, and D. J. Diekema. 2005. In vitro activities of anidulafungin against more than 2,500 clinical isolates of Candida spp., including 315 isolates resistant to fluconazole. *J. Clin. Microbiol.* 43: 5425–5427.
35. Tavanti, A., A. D. Davidson, M. J. Fordyce, N. A. Gow, M. C. Maiden, and F. C. Odds. 2005. Population structure and properties of *Candida albicans*, as determined by multilocus sequence typing. *J. Clin. Microbiol.* 43: 5601–5613.
36. Blystone, S. D., I. L. Graham, F. P. Lindberg, and E. J. Brown. 1994. Integrin alpha v beta 3 differentially regulates adhesive and phagocytic functions of the fibronectin receptor alpha 5 beta 1. *J. Cell Biol.* 127: 1129–1137.
37. Gonzalez, A. M., R. Bhattacharya, G. W. deHart, and J. C. R. Jones. 2010. Transdominant regulation of integrin function: mechanisms of cross-talk. *Cell. Signal.* 22: 578–583.
38. Porter, J. C., and N. Hogg. 1997. Integrin cross-talk: activation of lymphocyte function-associated antigen-1 on human T cells alters alpha4beta1- and alpha5beta1-mediated function. *J. Cell Biol.* 138: 1437–1447.
39. Urban, C. F., U. Reichard, V. Brinkmann, and A. Zychlinsky. 2006. Neutrophil extracellular traps capture and kill *Candida albicans* yeast and hyphal forms. *Cell. Microbiol.* 8: 668–676.
40. Diamond, R. D., R. Krzesicki, B. Epstein, and W. Jao. 1978. Damage to hyphal forms of fungi by human leukocytes in vitro. A possible host defense mechanism in aspergillosis and mucormycosis. *Am. J. Pathol.* 91: 313–328.
41. Harler, M. B., E. Wakshull, E. J. Filardo, J. E. Albina, and J. S. Reichner. 1999. Promotion of neutrophil chemotaxis through differential regulation of beta 1 and beta 2 integrins. *J. Immunol.* 162: 6792–6799.
42. Lerman, Y. V., K. Lim, Y. M. Hyun, K. L. Falkner, H. Yang, A. P. Pietropaoli, A. Sonnenberg, P. P. Sarangi, and M. Kim. 2014. Sepsis lethality through exacerbated tissue infiltration and TLR-induced cytokine production by neutrophils is dependent on integrin alpha3beta1. *Blood* 124: 3515–3523.
43. Yipp, B. G., B. Petri, D. Salina, C. N. Jenne, B. N. Scott, L. D. Zbytnuik, K. Pittman, M. Asaduzzaman, K. Wu, H. C. Meijndert, et al. 2012. Infection-induced NETosis is a dynamic process involving neutrophil multitasking in vivo. *Nat. Med.* 18: 1386–1393.
44. Johansson, S., G. Svineng, K. Wennerberg, A. Armulik, and L. Lohikangas. 1997. Fibronectin-integrin interactions. *Front. Biosci.* 2: d126–d146.
45. Nagae, M., S. Re, E. Mihara, T. Nogi, Y. Sugita, and J. Takagi. 2012. Crystal structure of α5β1 integrin ectodomain: atomic details of the fibronectin receptor. *J. Cell Biol.* 197: 131–140.
46. Lavigne, L. M., X. M. O'Brien, M. Kim, J. W. Janowski, J. E. Albina, and J. S. Reichner. 2007. Integrin engagement mediates the human polymorphonuclear leukocyte response to a fungal pathogen-associated molecular pattern. *J. Immunol.* 178: 7276–7282.